纳米磁性材料进展

（都有为　南京大学物理系）

NanoMaterials

- **Nanometer-(nm)-The unit of length**
  1nm = 1 μ m/10^3 = 10^{-9} m. **1nm=10Å**
- **Nano-materials: At least, one dimension of object on the nanometer size scale, 1-100nm.**
- **Nanoparticle (0D), Nanowire (1D), Nanofilm (2D), Nanocrystallite(3D)**
- **Composites : At least one composition is nanomaterial.** **Nanoarchitectonics**

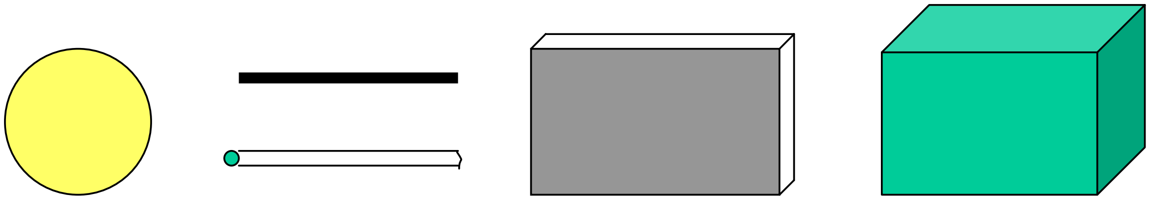

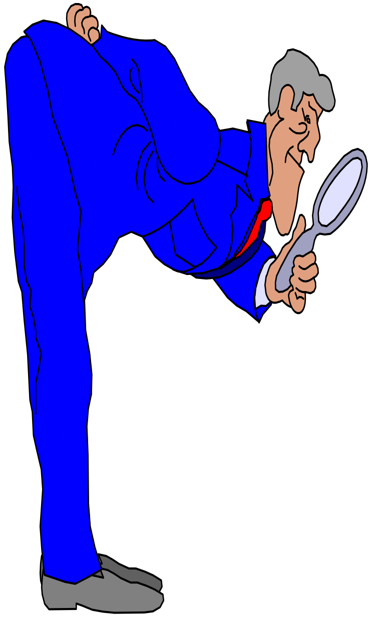

Characteristic Physical Length-L_{ch}

Magnetic single domain	10nm – 1 μ
Superparamagnetic	1 – 10nm
Exchange correlation length	10-40nm
Mean free path of electron	1 – 10nm
Spin diffusion length	10nm- 1 μ
Wave length of light	400/700nm

Small size effect; Quantum size effect;

MQT (Macroscopic quantum tunneling)

Surface effect $S_v = S/V \sim 1/d$

磁有序材料:

铁磁，亚铁磁,反铁磁

磁性材料:

永磁,高 Hc,高K

软磁,低 Hc,低K

磁记录,高Br

交叉耦合效应材料:

磁光,磁电,磁热,磁力

结构非灵敏性量:

Ms, Tc, K, λ,

结构灵敏性量:

Hc, Br, μ,

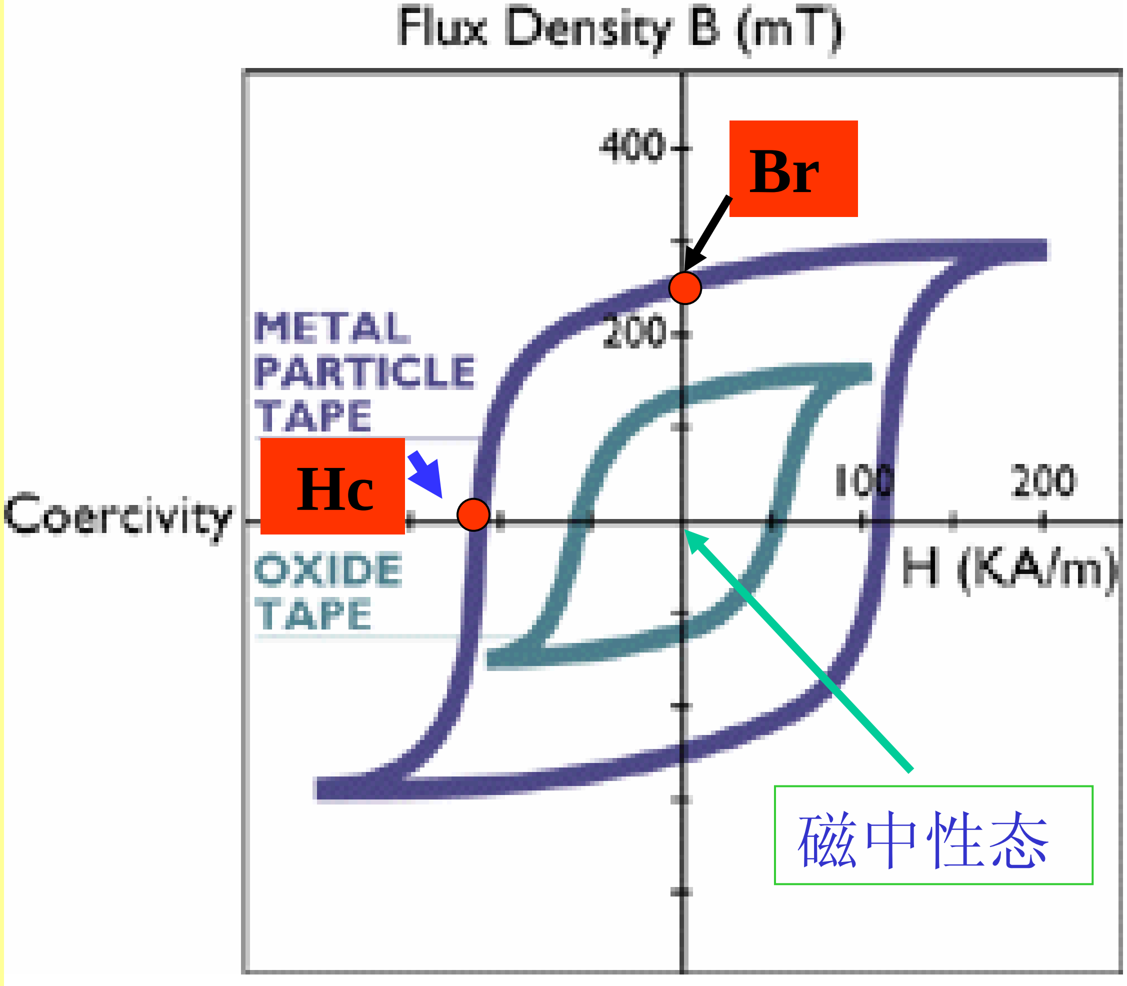

磁性材料(磁带)的磁滞回线

(Ⅰ).Magnetic Nano particles & Applications

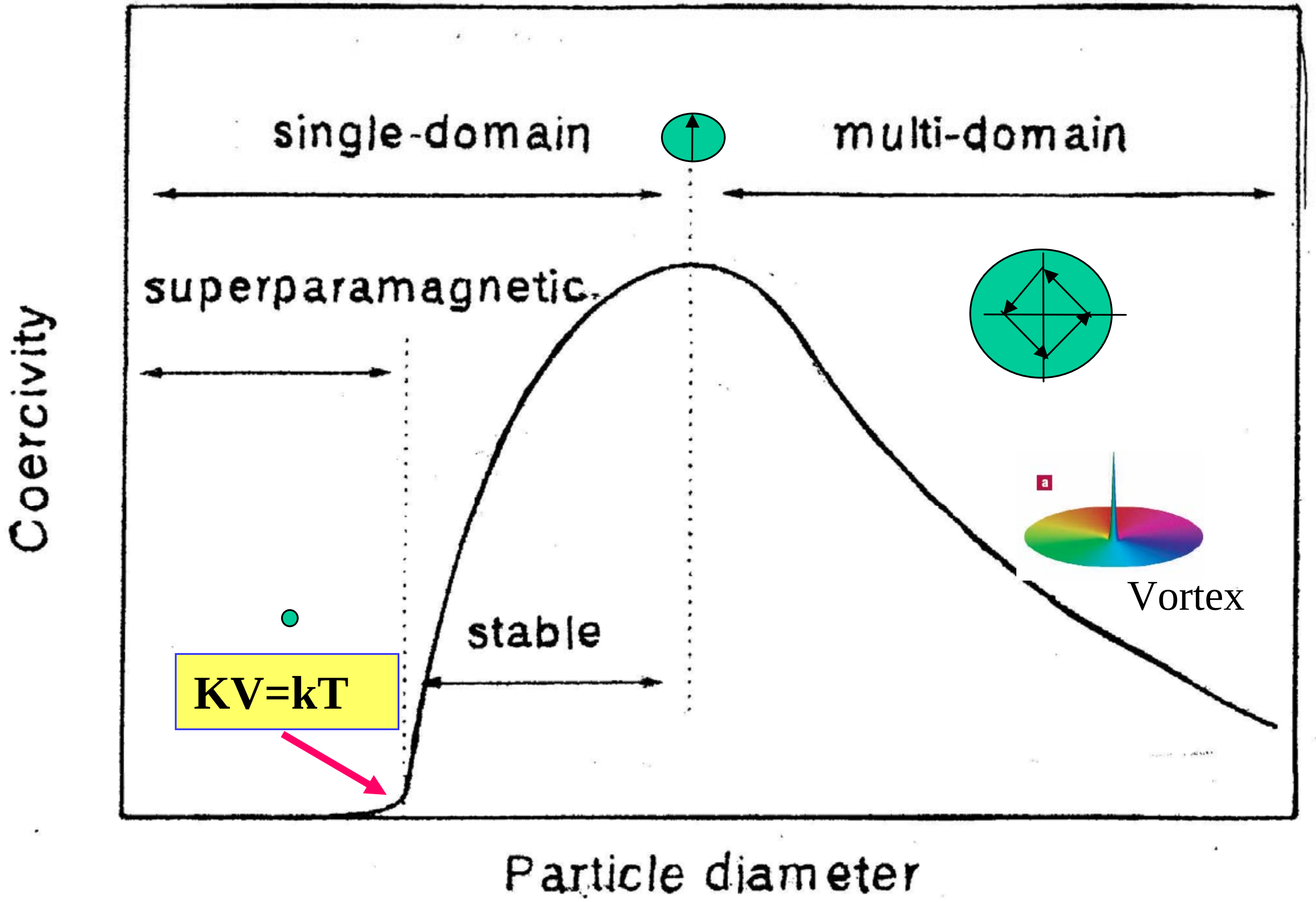

Fig. 1. Size dependence of coercivity.

The characteristic physical length

*** Single domain : $Rc \propto (AK)^{1/2}$**

M	Fe	Co	Ni	BaM	$Nb_2Fe_{14}B$	$SmCo_5$	$Sm_2Co_{17}N_{2.3}$
Rc (nm)	8.0	11.4	21.2	450	125	400	180

***Superparamagnetism: $KV=25k_BT_B$**

M	Fe_3O_4	Ni	Fe	Co
D(nm)	10	4.0	6.3	5
T_B(K)	300	25	78	55

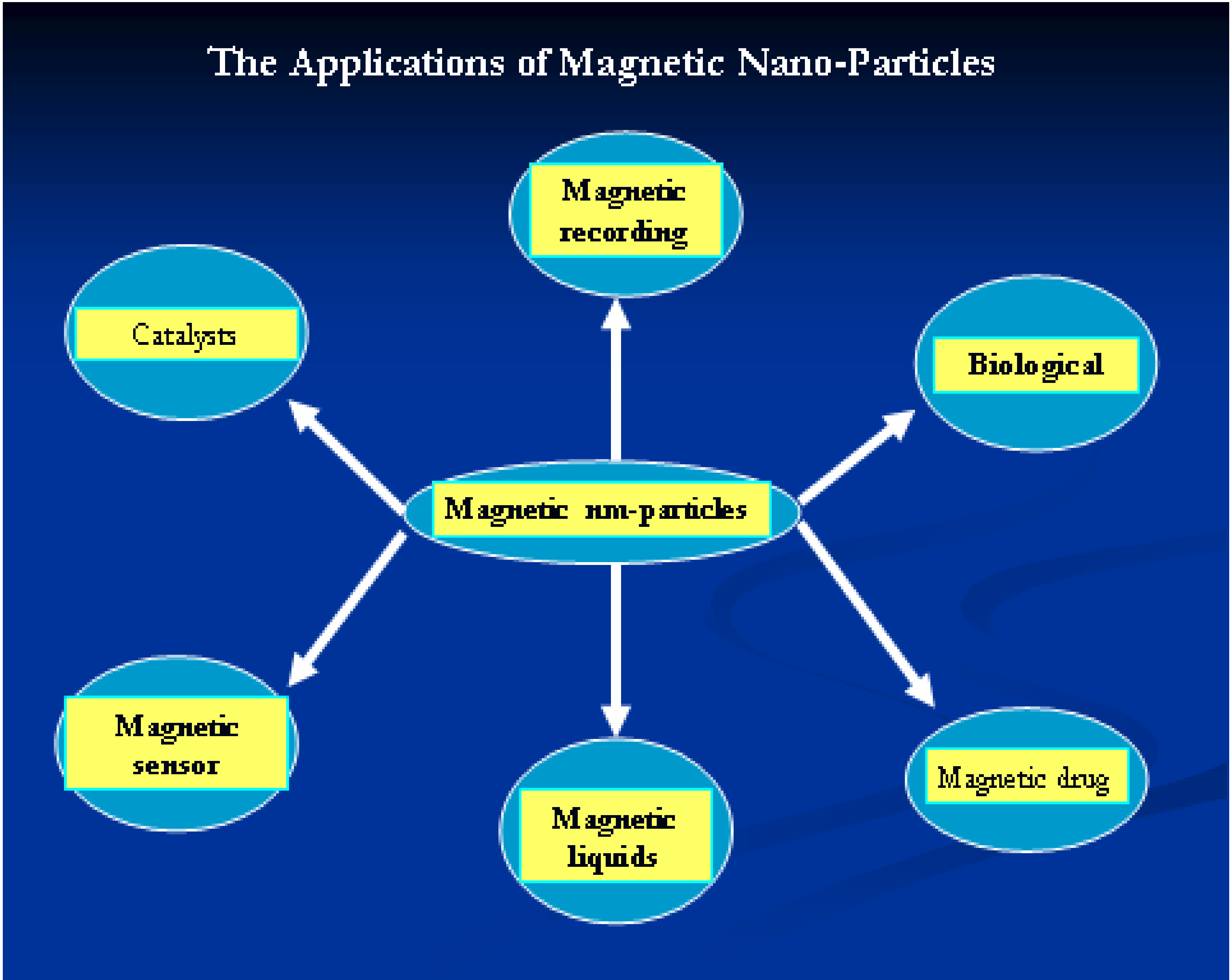

The Applications of Magnetic Nano-Particles
Magnetic recording
Catalysts
Biological
Magnetic nm-particles
Magnetic sensor
Magnetic liquids
Magnetic drug

Nanomedicine

Targeted drugs for lung cancer

The aerosols containing magnetic nanoparticles with drugs can be guided to specific regions in the lung of mice with an external magnetic field. With this technique, higher doses of drugs can be delivered to the cancerous region without increasing side effects.

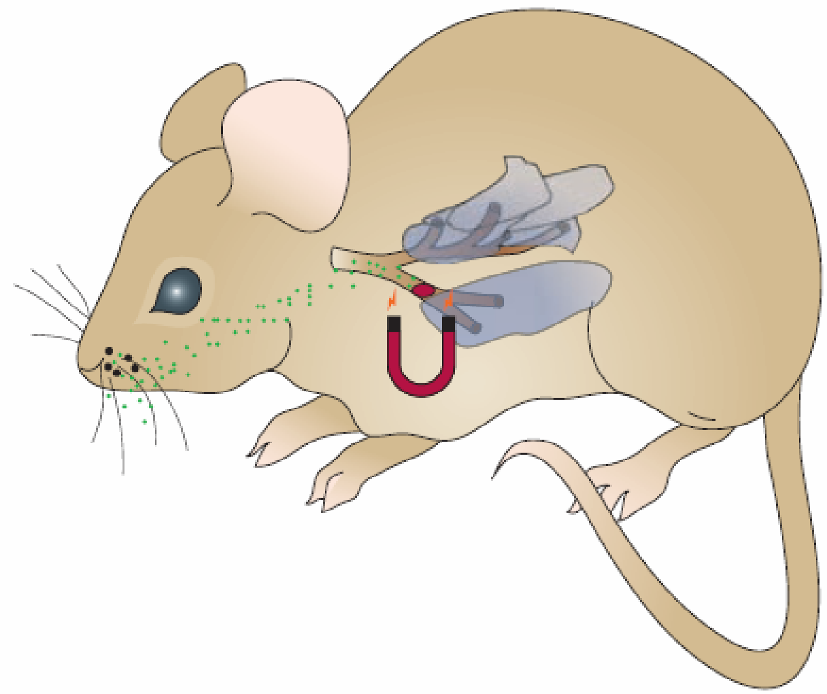

Figure 1 Magnetic-field guided drug delivery with magnetic aerosols. Superparamagnetic nanoparticles are placed in microdroplet aerosols (green) and delivered along the airways (brown) toward the lungs (grey). A localized magnetic field causes large numbers of nanoparticles to accumulate in a specific region, shown here in red.

P.Dames,et al., Nature Nanotech. 2(2007)495

A. Amirfazli Nature tecnology,2 (2007)467

Magnetotactic bacteria

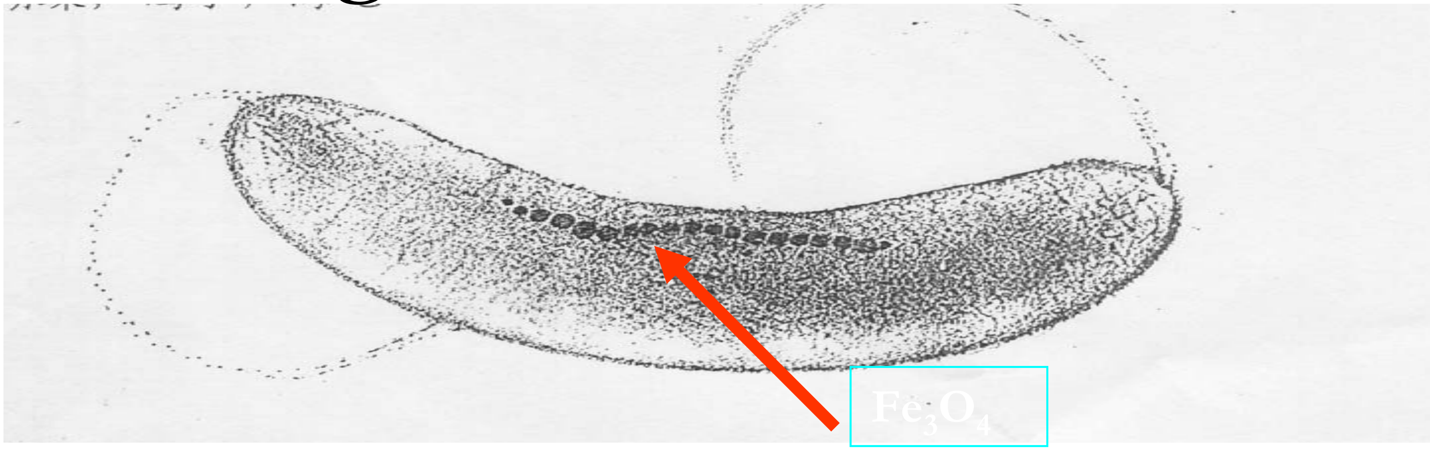

Magnetic nanochain assembled by magnetosome

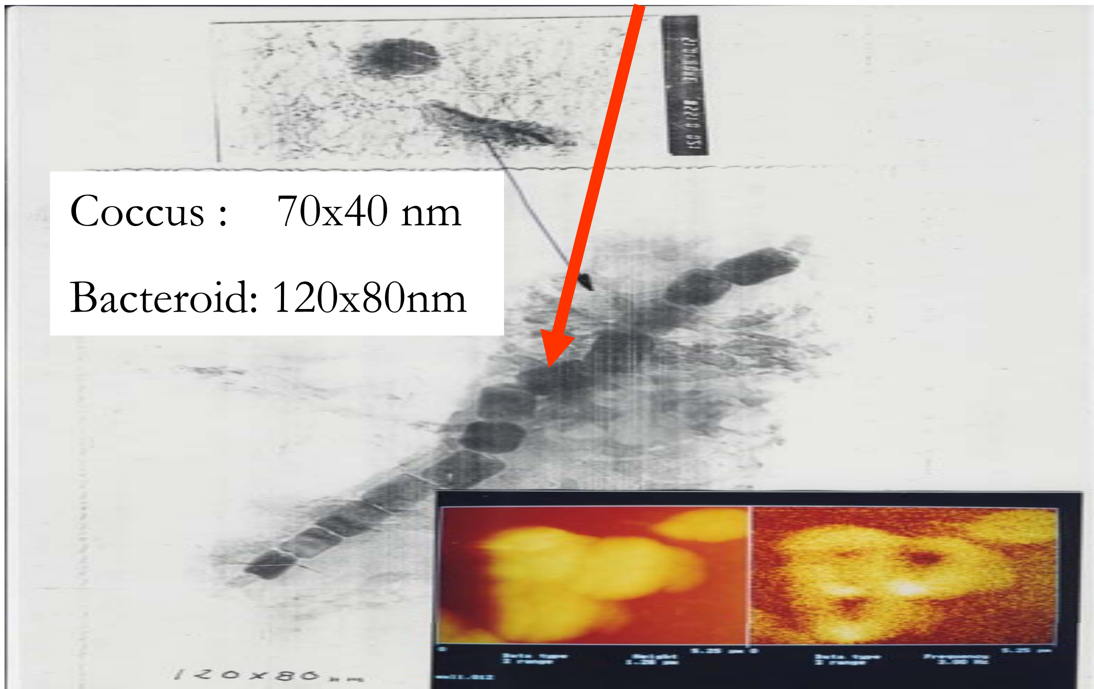

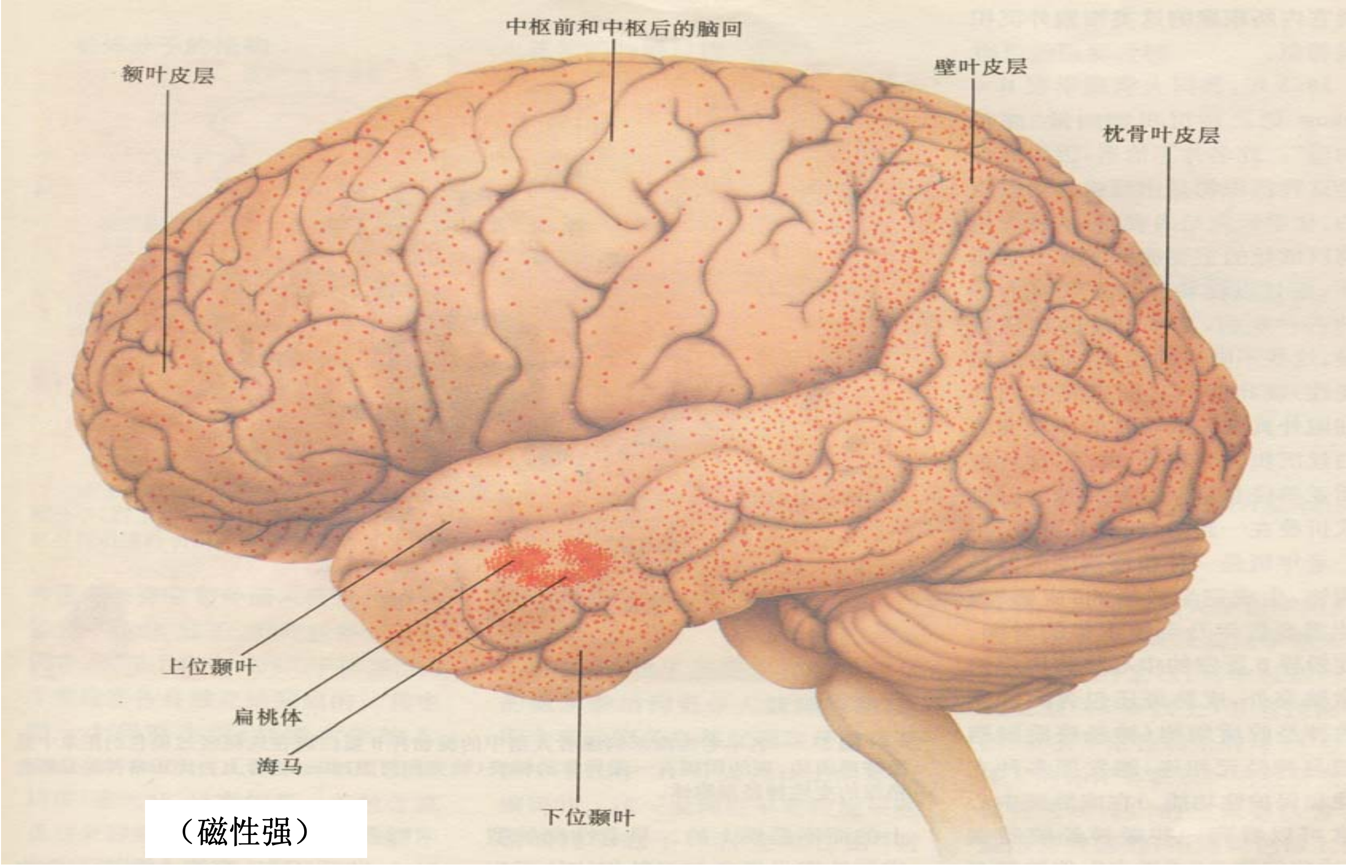

每克人脑中至少存在500万颗磁铁矿纳米微粒，支配记忆部分是海马，保管记忆是颞叶。猴子没有明显磁性

The first product in nano-materials is "Ferrofluid" in 1965.

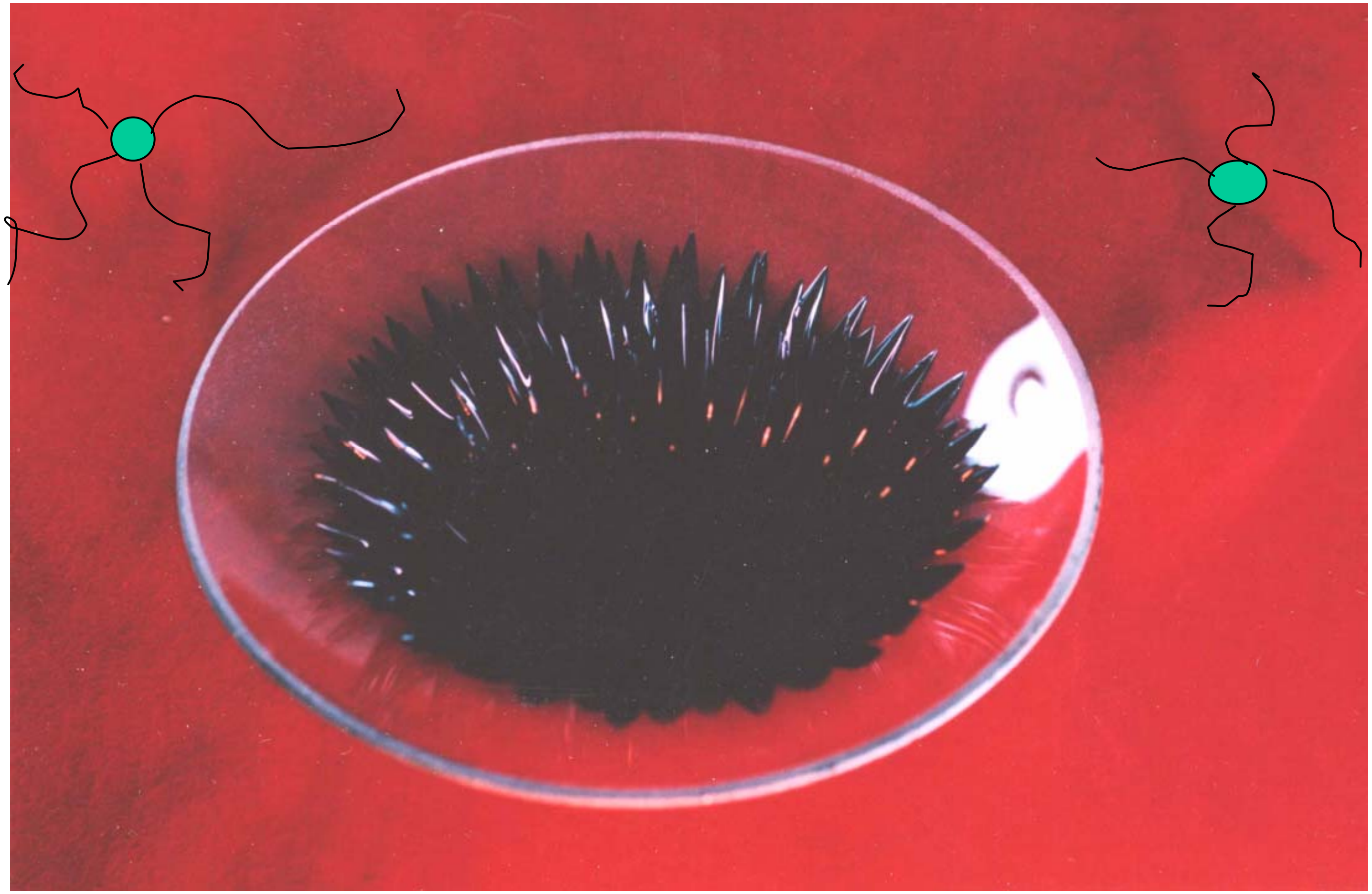

Magnetic liquid(Fe_3O_4)

Interface for magnetic particles with Core/shell structure

- **Antiferromagnet (AFM) / Magnetic particle**
- **Ferromagnet (FM) or Ferrimagnet (FIM)/ Magnetic particle**
- **Nonmagnetic organic, Inorganic or metal /Magnetic particle**

The functions of the shell

1. **To control the magnetic properties**
2. **To prevent grain growth and agglomeration**
3. **To enhance chemical stability**
4. **To get some exchange couple effect**

Exchange couple in (Co/CoO) nanoparticles

a). Hysteresis loops at 77K of CoO/Co particles.

(1). After cooling the sample in a 10kOe field. (2).ZFC

$$F = HM_S \cos\theta - K_U \cos\theta + K_1 \sin^2\theta,$$

K_U – **unidirectional anisotropy energy constants.**

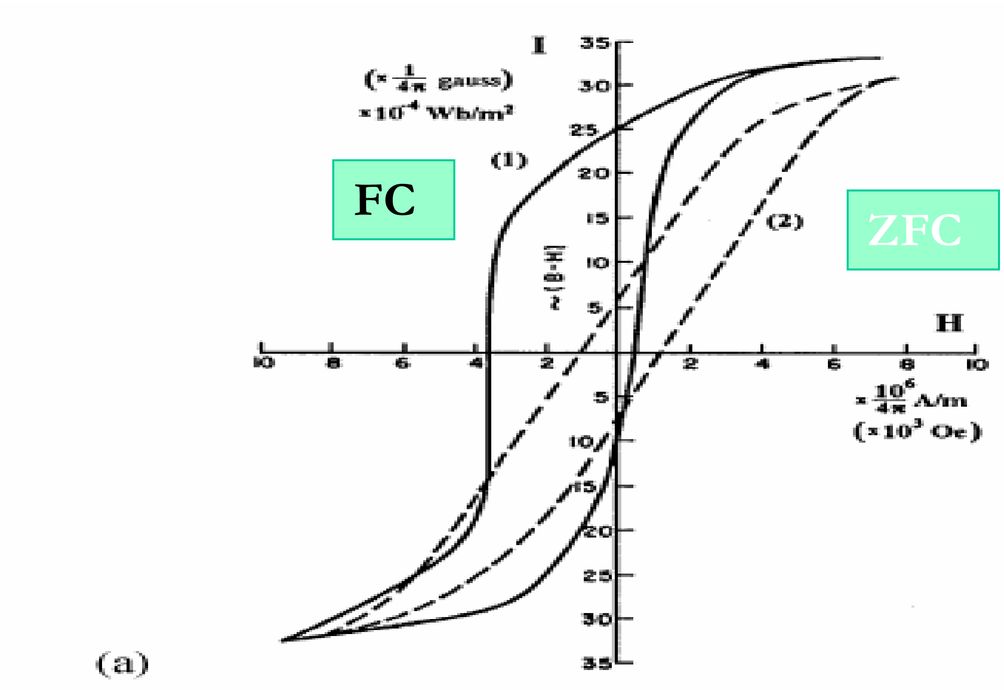

FM/AFM

Co/CoO

T_N=293K

W.H.Meiklejohn, C.P.Bean, Phys.Rev. 102(1956)1413; 105(1957) 904.

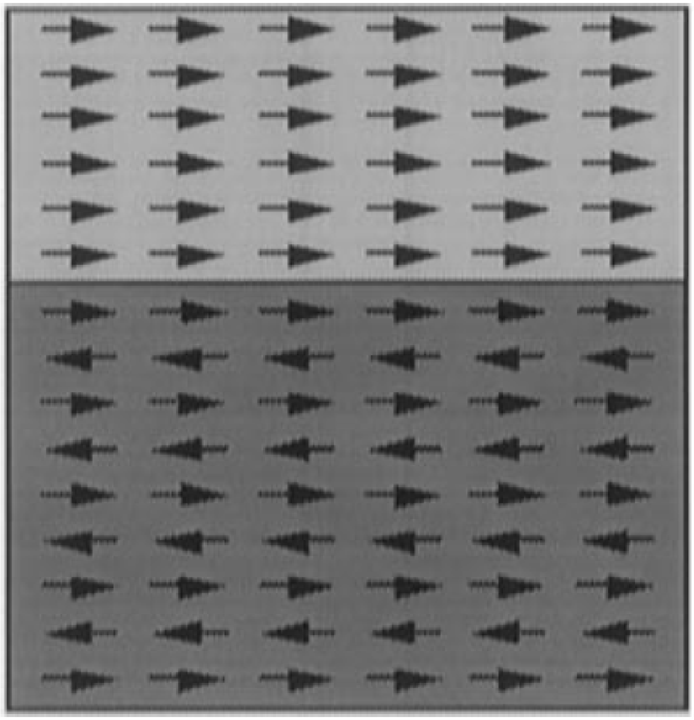

Schematic of the ideal FM/AFM interface

$$H_E = \frac{\Delta\sigma}{M_{FM} t_{FM}} = \frac{2J_{ex} S_{FM} \cdot S_{AFM}}{a^2 M_{FM} t_{FM}},$$

	CoO	NiO	CuO	Ir-Mn	Pt-Mn	Rh-Mn	Fe-Mn
T_N(K)	293	525	453	**600-750**	**485-975**	**850**	**425-525**

The surface spin of antiferromagnet can either be compensated (the magnetic moments with the atomic surface layer cancel out) or uncompensated

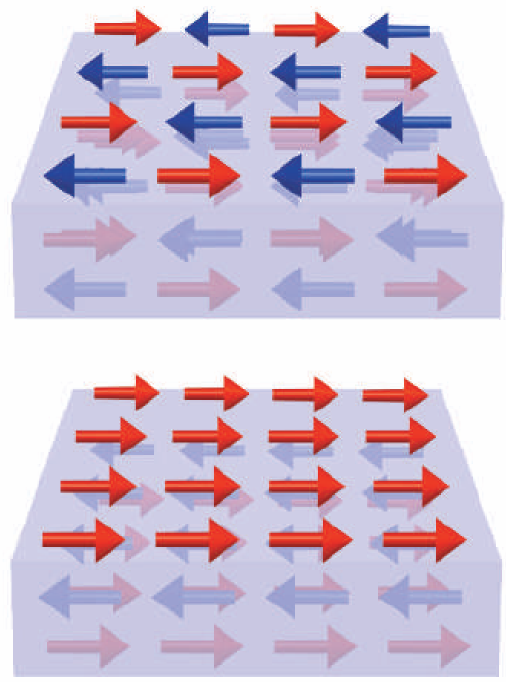

Figure 1 Compensated (top) and uncompensated (bottom) antiferromagnetic surfaces

Figure 2 Growth steps on the surface of a compensated antiferromagnet as a consequence of steps in the underlying ferromagnetic layer (yellow). The angled step on the right is uncompensated due to the red, right-pointing spins being present at the top as well as bottom of the step.

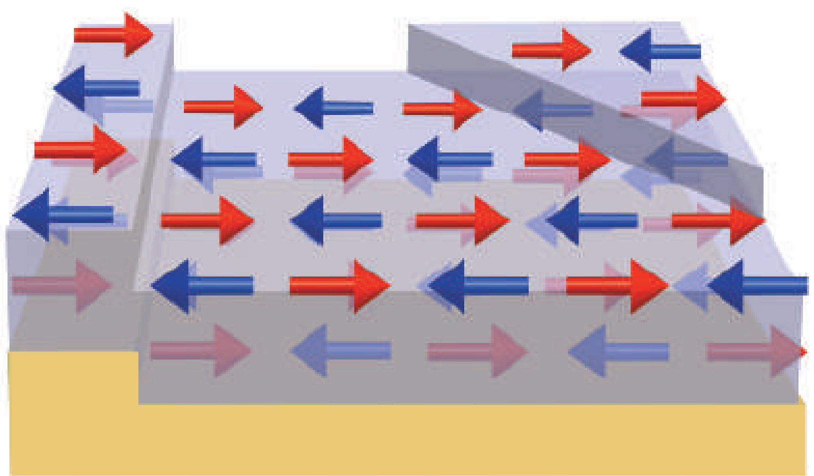

Kuch W. et al.Nature Material 5(2006)128; Blamire M. and Hickey B.ibid,5(2006)87

Beating the superparamagnetic limit with exchange bias

The blocking temperature ,T_B , increases almost two orders magnitude for 4nm Co/CoO nano particles in the CoO matrix. This leads to a marked improvement in thermal stability. This mechanism provides a way to beat the superparamagnetic limit in isolated particles.

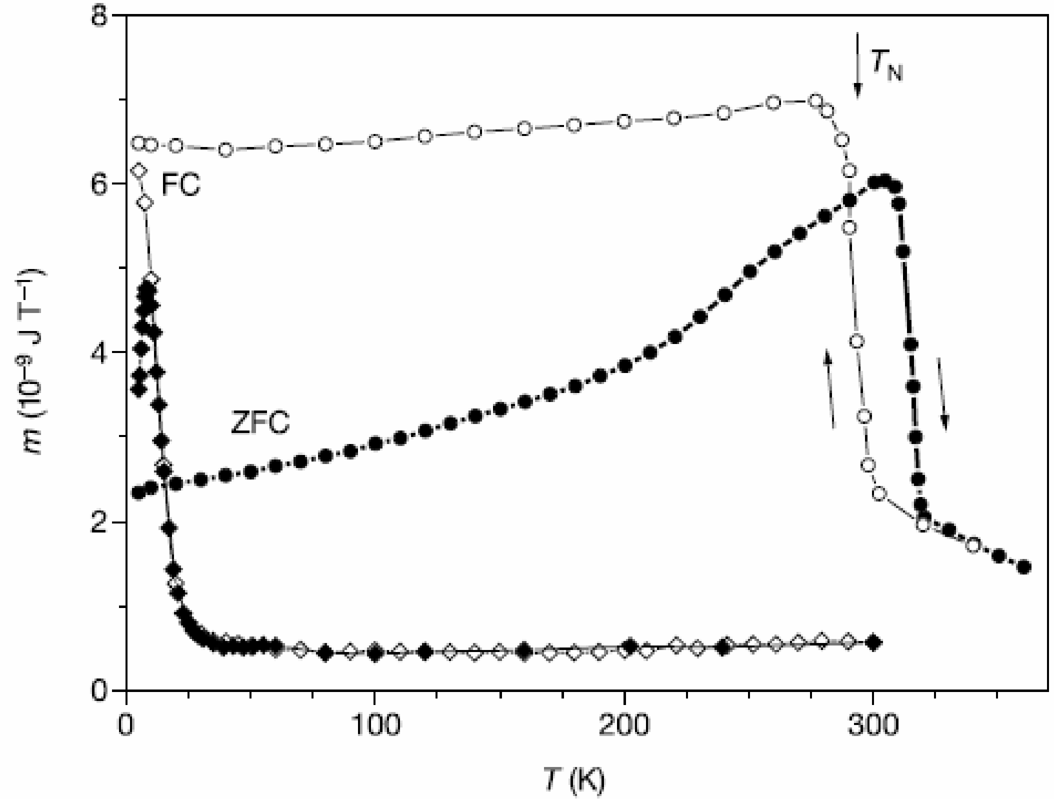

Figure 2 Magnetic moments of 4-nm $Co_{core}CoO_{shell}$ particles. Shown is the temperature dependence of the zero-field cooled (ZFC; filled symbols) and field-cooled (FC; $\mu_0 H_{FC} = 0.01$ T, open symbols) magnetic moment (m) of 4-nm $Co_{core}CoO_{shell}$ particles. Particles were embedded in a paramagnetic (Al_2O_3) matrix (diamonds), or in an AFM (CoO) matrix (circles). The measuring field is $\mu_0 H = 0.01$ T. The Néel temperature of CoO is indicated by an arrow. The lines are guides to the eye.

V. Skumryev et al., Nature 423 (2003)850

The main research works in our group

1. Hard ferrite $SrFe_{12}O_{19}$ particles

   coated by CoO, γ - Fe_2O_3, Fe_3O_4.

2. Soft magnetic metal particles

   (Fe, FeNi) coated with Al_2O_3, SiO_2 and

   SiO_2 /C,

1. $SrFe_{12}O_{19}$ / CoO

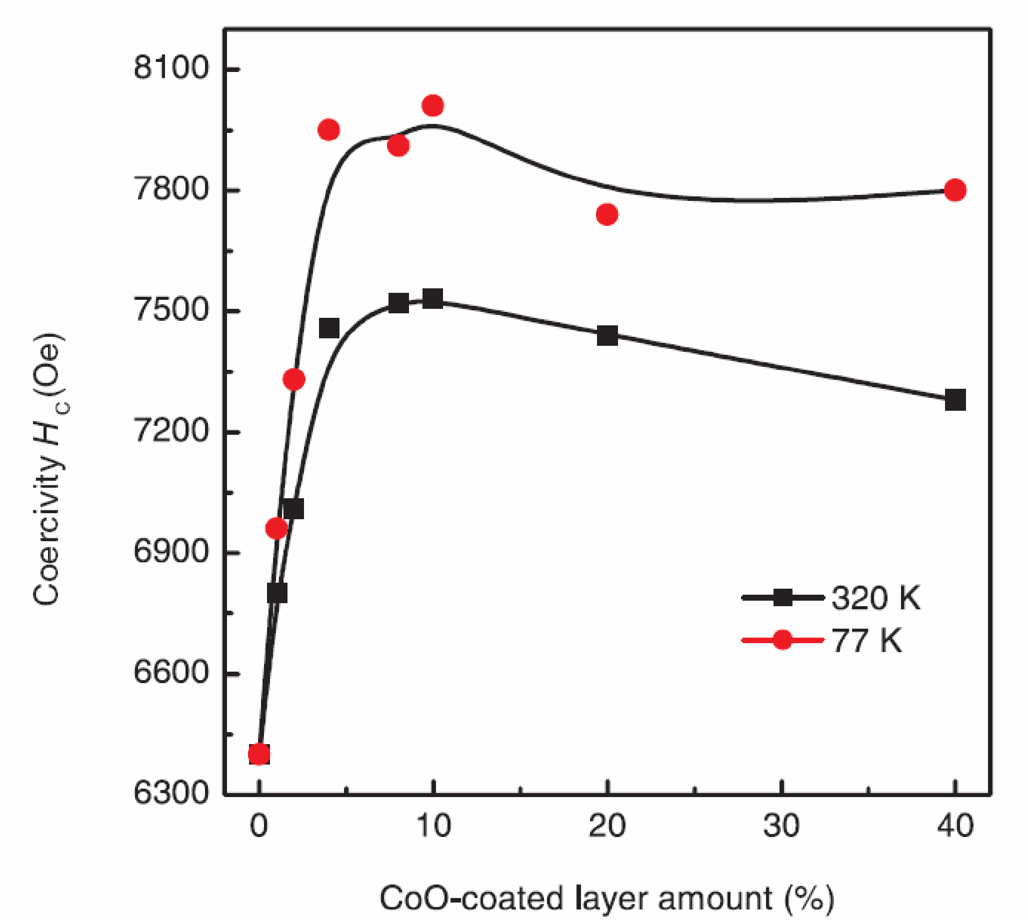

Hc sharply increases for small CoO content, then reaches a maximum at 10% of the coating amount

Liu XS et al., Appl. Phys. A 77 (2003)673

2. SrM / Fe3O4

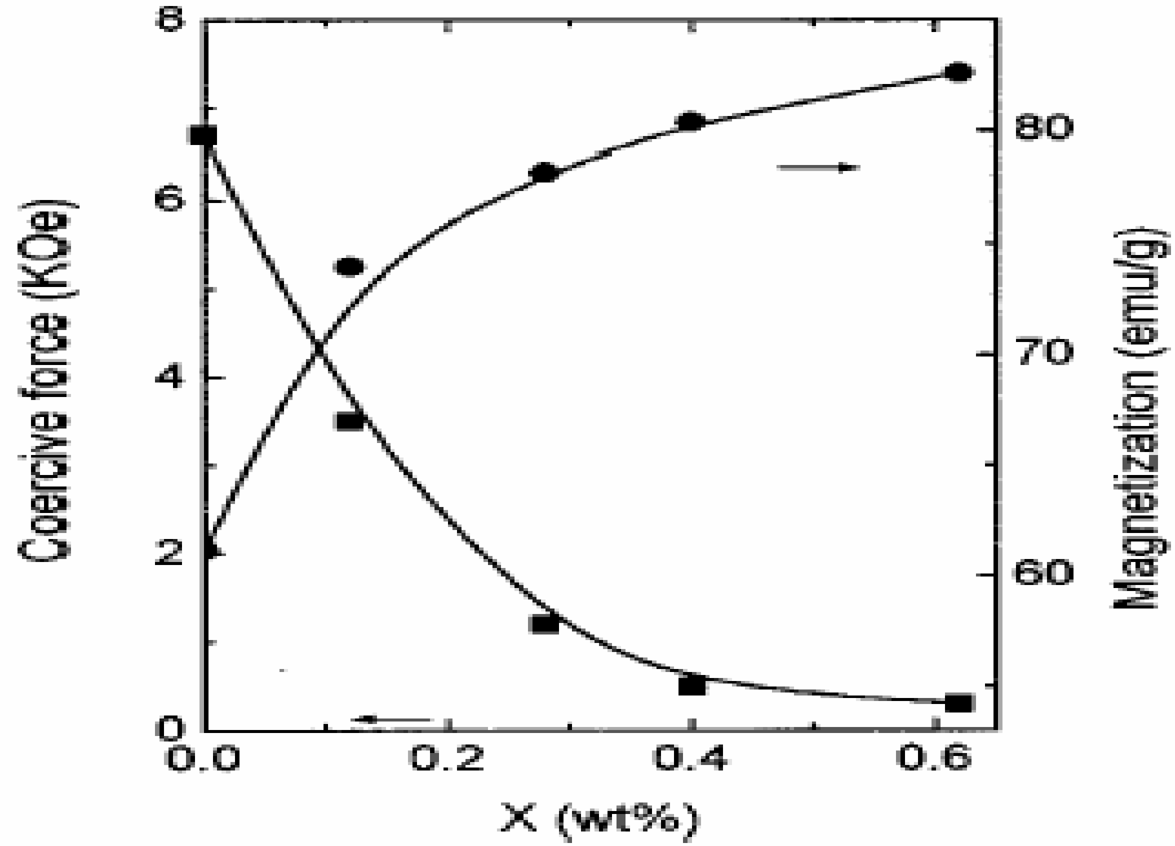

SrM particles coated with soft magnetic materials Fe3O4 , Ms increases and Hc decreases very obviously with the rise of Fe3O4 coating . The Hc can be controlled by coated quantity.

3. $Fe/SiO_2/C$

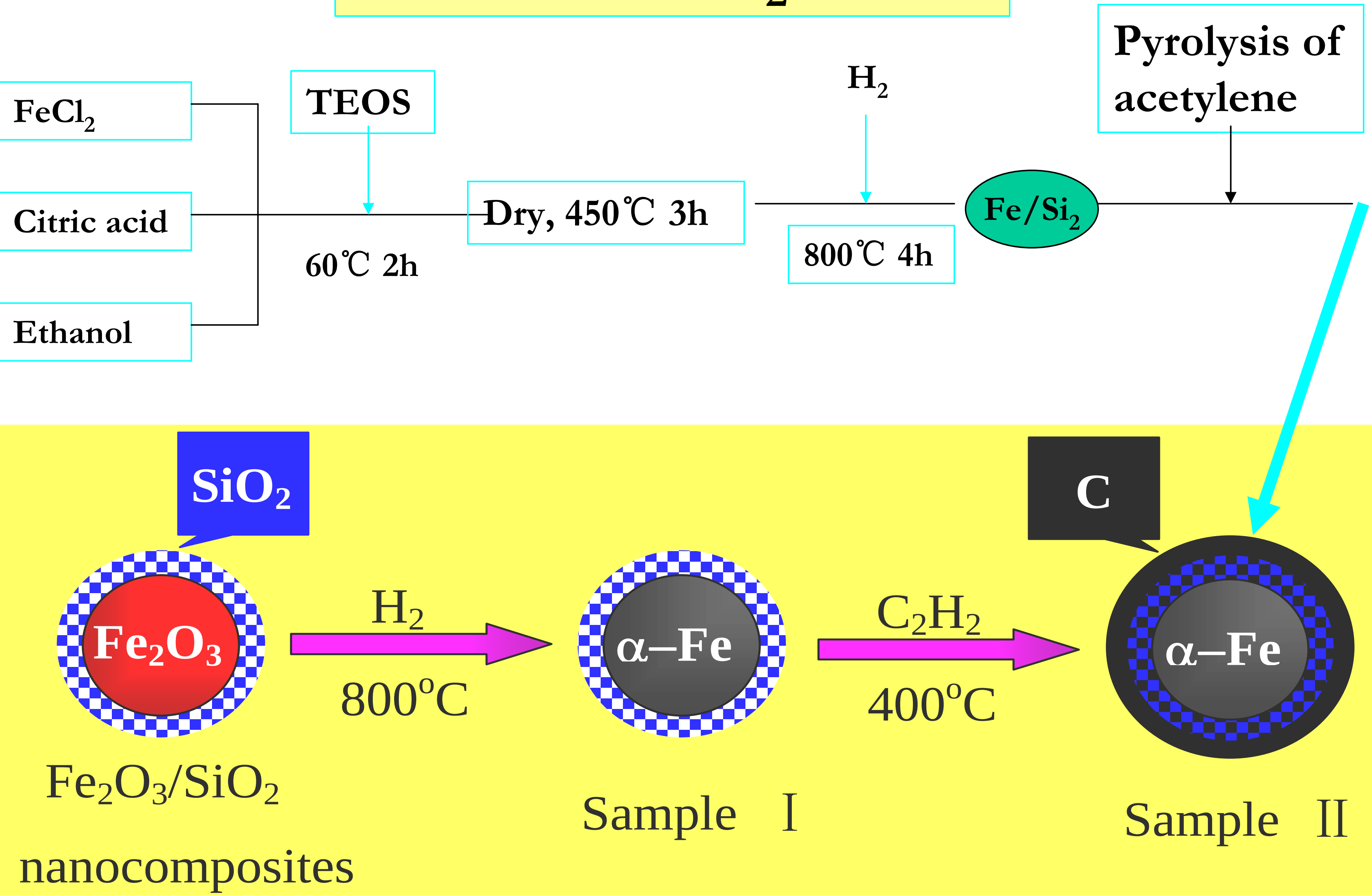

$FeCl_2$
Citric acid
Ethanol
TEOS
60℃ 2h
Dry, 450℃ 3h
H_2
800℃ 4h
Fe/Si_2
Pyrolysis of acetylene
SiO_2
Fe_2O_3
H_2
800^{o}C
α–Fe
C_2H_2
400^{o}C
C
α–Fe
Fe_2O_3/SiO_2 nanocomposites
Sample Ⅰ
Sample Ⅱ

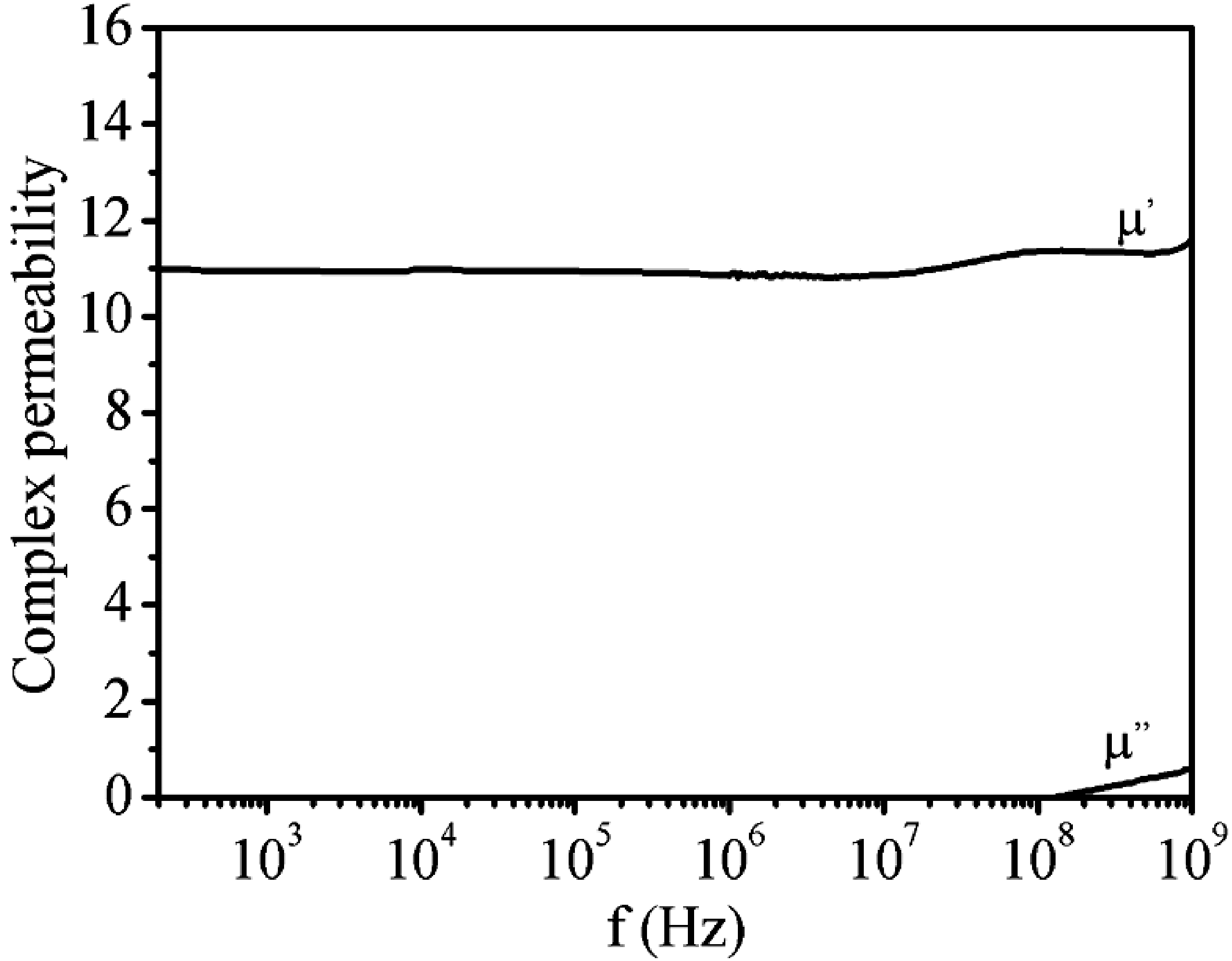

The permeability spectra of （ Fe/SiO_2 /C） particles sample at room temperature。

N.J. Tang et al., Carbon 44(2006)423

（Ⅱ). Magnetic Nanocrystalline Materials

- The nanocrystalline material is composed of nanocrystallines. It may be considered as a densely assembly of nano-particles which are interacted through interface.
- Huge interface
- Interaction
- Exchange interaction
- Magnetic interaction

Exchange length , $L_{ex}=(A/Ms^2)^{1/2}$. (within L_{ex} the spins of ferromagnet remain parallel, L_{ex} 1-6 nm)

Domain wall width, $\pi\ \delta_o$,

$\delta_o = (A/K)^{1/2}$. **(exchange correlation length or domain wall parameter, the distance over which the variations of the spin orientation are correlated)**

$\delta_o \approx L_{ex}$ **(for hard magnets, while , $\delta_o >> L_{ex}$ for soft magnetic materials)**

Single domain size for a sphere, $R_{SD}=(AK)^{1/2}$

	L_{ex}(nm)	$\pi\ \delta$ o(nm)	D_{SD}(nm)	J. Nogués et al., Physics Reports, 422(2005)65-117
Fe	1.5	40	18	
Co(hcp)	2.0	12	70	
Ni	3.4	80	60	
$Ni_{80}Fe_{20}$	4.0	100	22	
$SmCo_5$	4.9	4.0	764	

(2.1). Nano-Crystalline Soft Magnetic Materials

- **The progress of soft magnetic materials**
- **Fe**
- **→ FeSi(1900)**
- **→ FeNi(1920)**
- **→ Ferrites (1935-1946)**
- **→Amorphous (1970)**
- **→ Nano-Crystalline Soft Materials**

Magnetic nanocrystalline system. FM/FM interface

Random anisotropy theory---Herzer JMMM.294(2005)99

$Lo=(A/K)^{1/2}$, If D< Lo,
$Ke = K/N^{1/2}$,
$N=(Lo/D)^3$,
$Hc \sim D^6$,

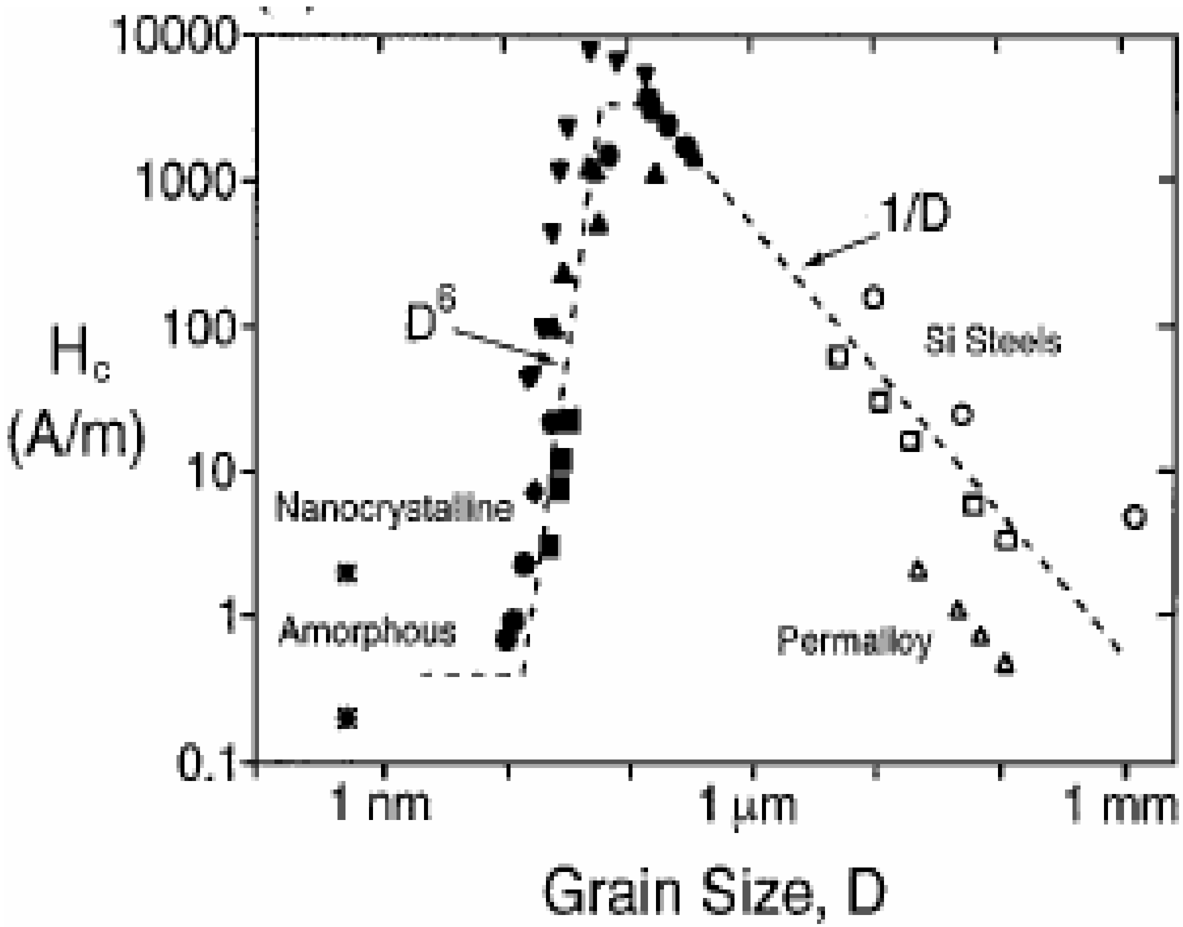

M	α -Fe	α $-Fe_{amr}$	$Nd_2Fe_{14}B$	$SmCo_5$	$Sm_2Fe_{17}N$
L_o(nm)	23	35	2.1	5.2	2.6

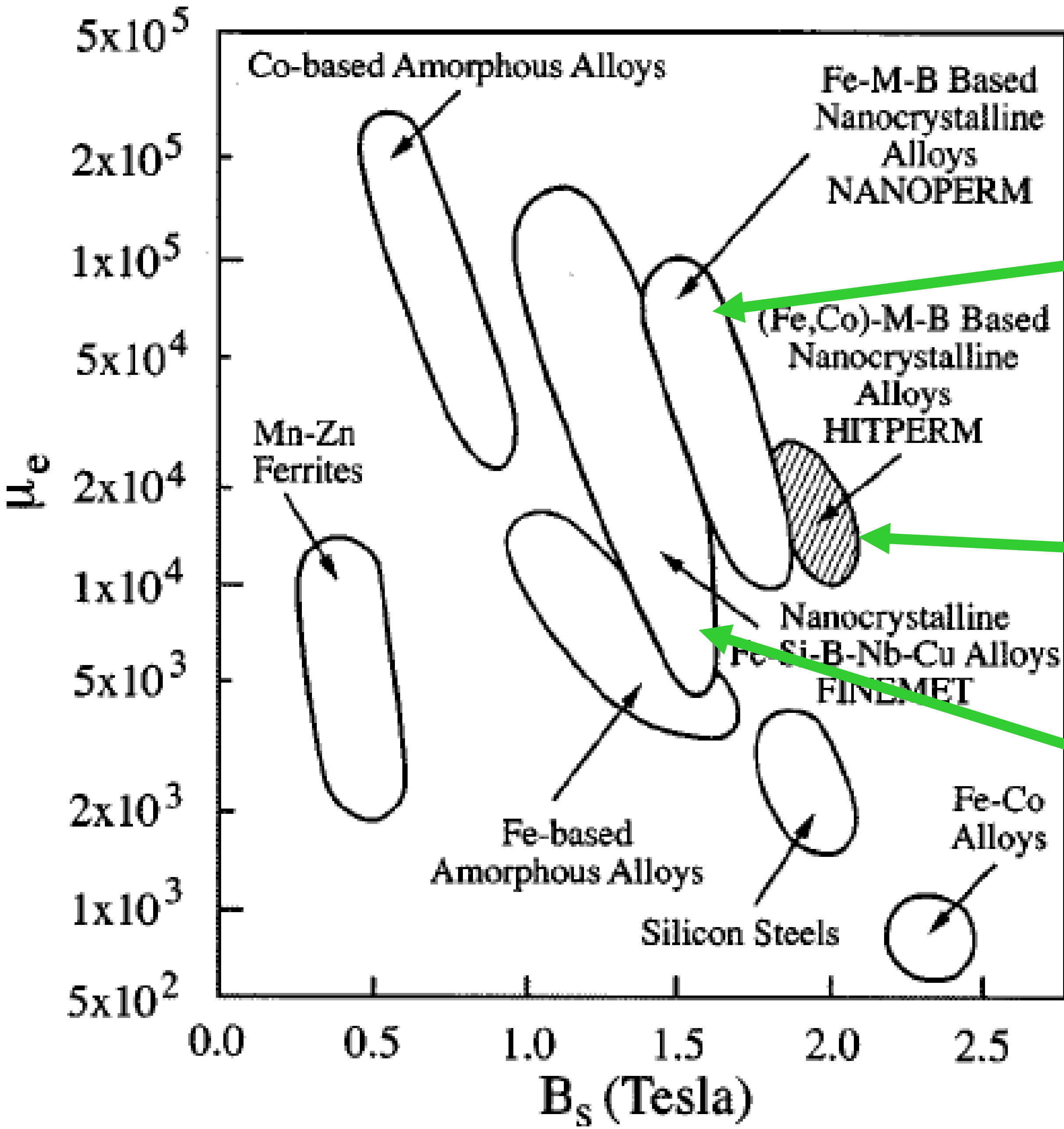

Commercial Nanocrystlline Alloy

2. NANOPERM
Fe-M-B-Cu
(M=Zr,Nb,Hf--)

3. HITPERM
(FeCo)-M-B-Cu

1. Finemet (1988)
Fe73.5Si13.5B9Nb3Cu1

(2.2). Nanocomposite exchange coupled magnets

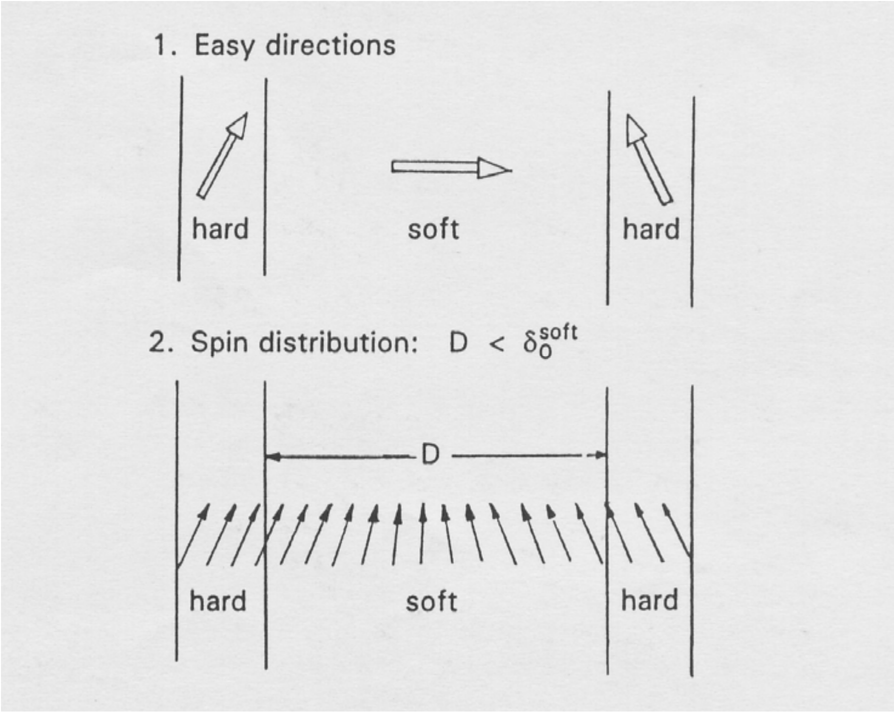

Remanence:

Mr/Ms>1/2

Reduced the quantity of rare earth element

Ms;Tc;K for some soft and hard magnetic materials

	Fe	Ni	Co	Fe_2Co	SrM	NdFeB
Ms(kA/m)	1714	484	1422	1933	370	1281
Tc (K)	1043	631	1404		733	585
K(kj/m^3)	42	-51	530		370	4400

- Saturation magetization Ms: Hard < soft
- Anisotropy K : Hard > Soft
- Nanocomposity exchange coupled of hard and soft phases maybe have both high Ms and Hc
- (BH)m=1 MJ/m3 (120 MG Oe), RE~5 wt %. for 2.4 nm $(Sm2Fe17N)_3$ /9 nm $(Fe_{65}Co)_{35}$

R.Skomski and J.M.D.Coey, Phys.Rev.B 48(1993)15812

The best magnetic properties for $(Nd,Pr,Dy)_2Fe_{14}B/\alpha$-Fe

B_r=1.438T(14.38kG)

H_{cj}=995KA/m (12.5kOe)

$(BH)_m$=405KJ/m3 (50.97MGOe)

DAYTON University

Lee D et al.,Proc. Of 18thInternational Workshop on HPMA(Annecy, france,August-September,2004).Vol. 2, 667-9\678

Nanocomposite exchange coupled is diffusing to other applications:

1。Magnetic recording : FePt/FeRh reduced reversely field

2。Magnetostriction : TbFe/Fe (FeCo) multylayer，reduced Hc

（III）Magnetic Nanowire & Nanotube

- Magnetic nanowires have various applications such as: perpendicular magnetic recording media for high density magnetic recording.
- Sensor in MEMS
- Magnetic multilayered nanowires for CPP-GMR
- The spin diffusion length can be determined.

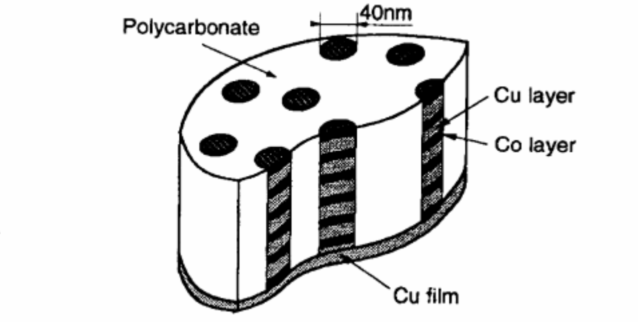

Fig. 1. Schematic of an array of multilayered nanowires in nanoporous track-etched polymer membrane.

SUL-Soft magnetic underlayer

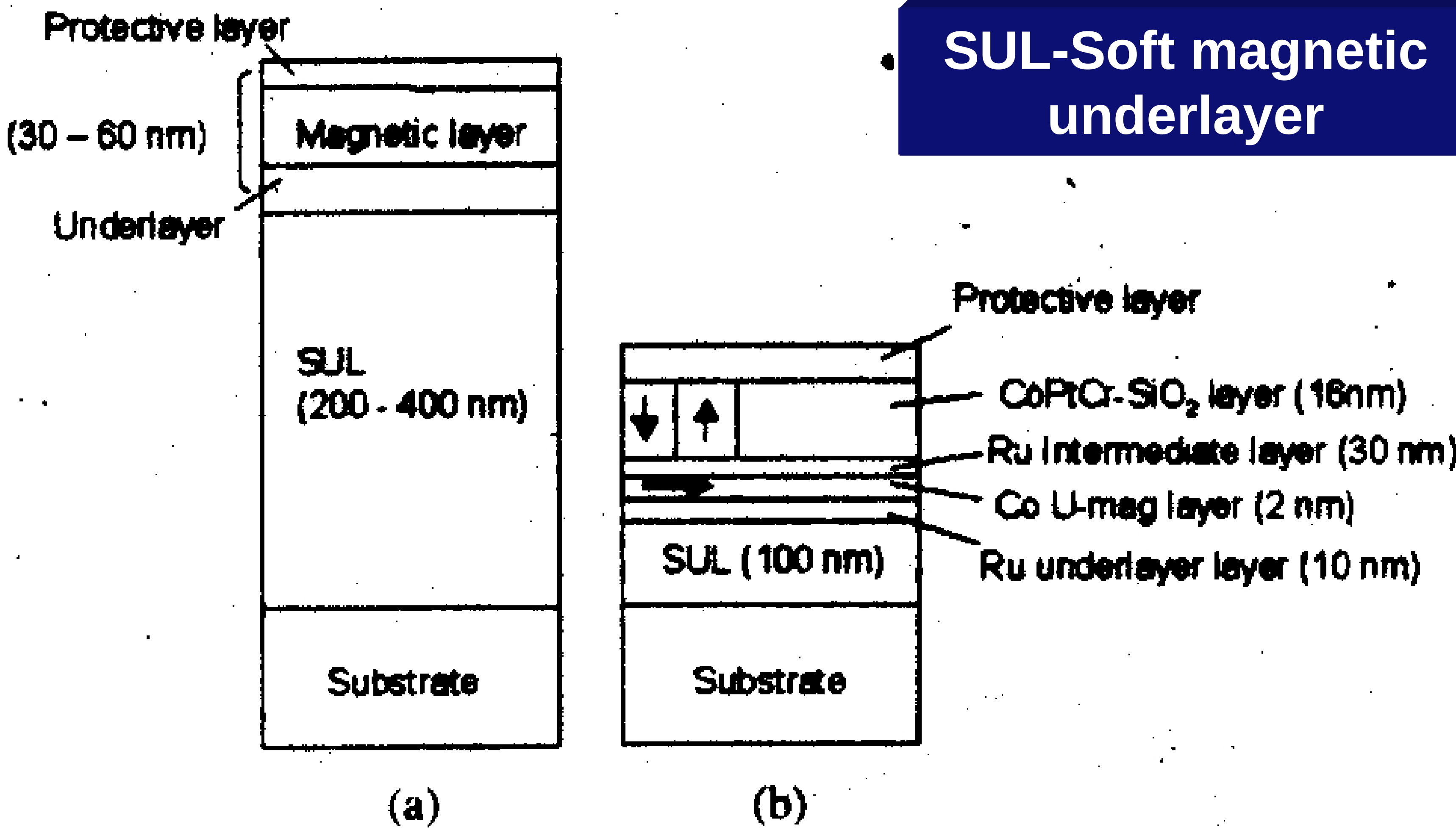

Fig. 1. Cross-sectional structures of (a) a conventional perpendicular recording and (b) the U-mag media.

Longitudinal to Perpendicular Magnetic Recording model.

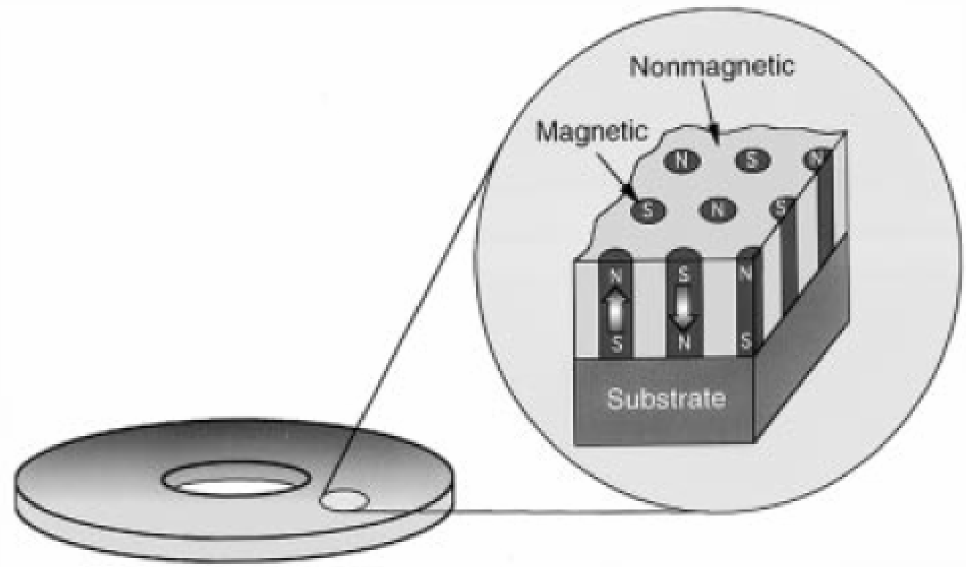

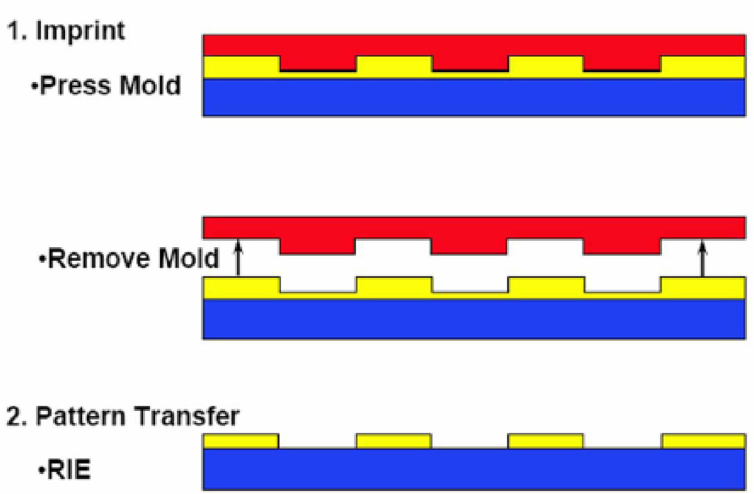

Bit –Patterned media (Quantized magnetic disk)

Patterned magnetic nanostructures give us new freedom in controlling magnetic material properties.

Schematic of nanoimprint lithography consisting of 1).imprint and 2). pattern transfer

For mass production

S.Y. Chou Proceedings of the IEEE85(1997)652

R.F.Pease and S.Y. Chou ,Proceedings of the IEEE96(2008)248

Tilted magnetic media

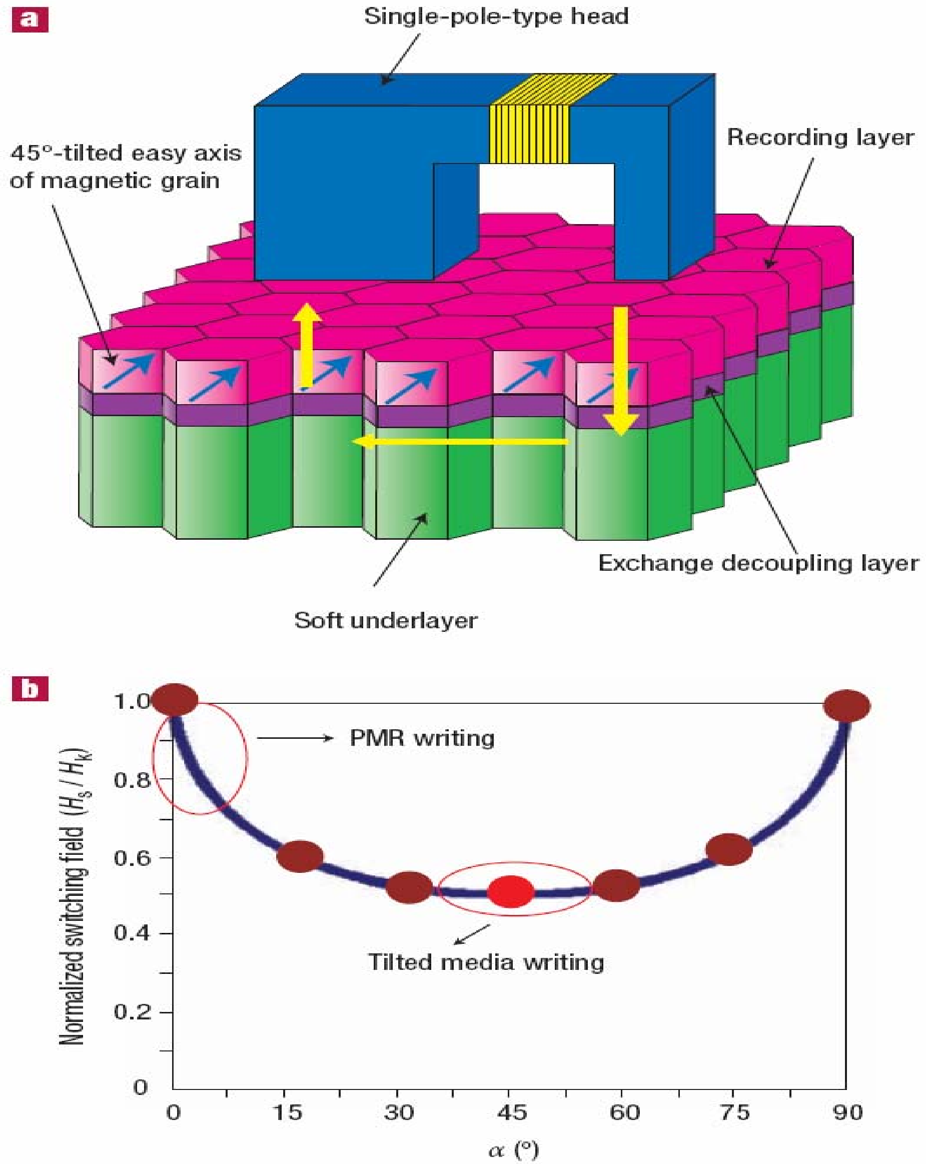

Figure 1 Tilted magnetic media. **a**, A perpendicular recording system with a single-pole-type writing head and a 45°-tilted medium. The yellow arrows indicate the magnetic flux from pole to pole. (Not to scale. Magnetic grain size should be around 5 nm for 1 Terabit in^{-2} recording. The single pole dimension will be around 80 nm or less.) **b**, Switching-field distribution versus angle (α) between the external field and easy axis of a single Stoner–Wohlfarth grain. It appears that low noise (exchange-decoupled) thin-film media would follow the Stoner–Wohlfarth switching model (uniform magnetization reversal): $H_s = 1/\{(\cos^{2/3}\alpha + \sin^{2/3}\alpha)^{2/3}\}$.

J.P.Wang,Nature Materials4 (2005)191

The main research works in our group

(Anodic alumina oxide AAO template)

1.Nanowires: Fe, Ni, Co, Pb and FeCo ,

2. Co/Pb, Ni/Pb, Fe/Pb, FePt/Fe

2.Nanotubes :$CoFe_2O_4$; $CoFe_2O_4/Pb(Zr,Ti)O_3$

3.Helical carbon nanotubes

$Fe_{48}C0_{52}$ nmwires

Porous alumina template

D~22nm

Interpore distance~ 50nm

Hc=3.89 kOe

Mr/Ms=0.954

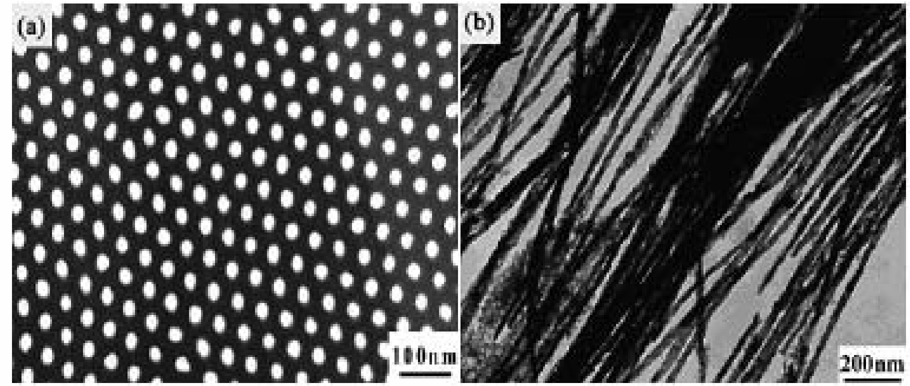

Figure 1. TEM images of (a) a porous alumina template with an interpore distance of about 50 nm and (b) typical $Fe_{48}Co_{52}$ nanowires with a diameter of about 22 nm.

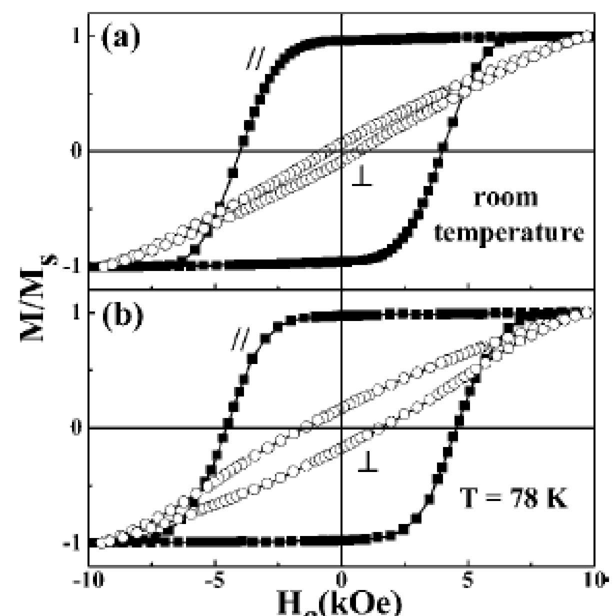

Figure 5. Hysteresis loops of the arrays with a diameter of about 22 nm and an interpore distance of about 50 nm measured at room temperature (a) and at 78 K (b).

H .L Su et al., Nanotechnology 16(2005)429

Co-Pb heterogeneous alloy nanowire arrays

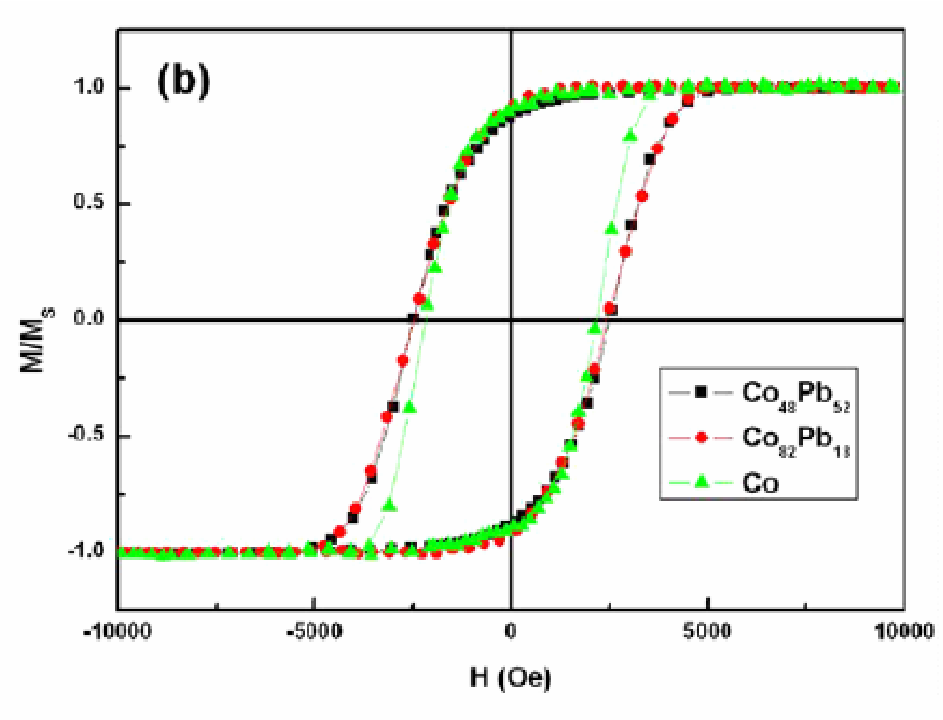

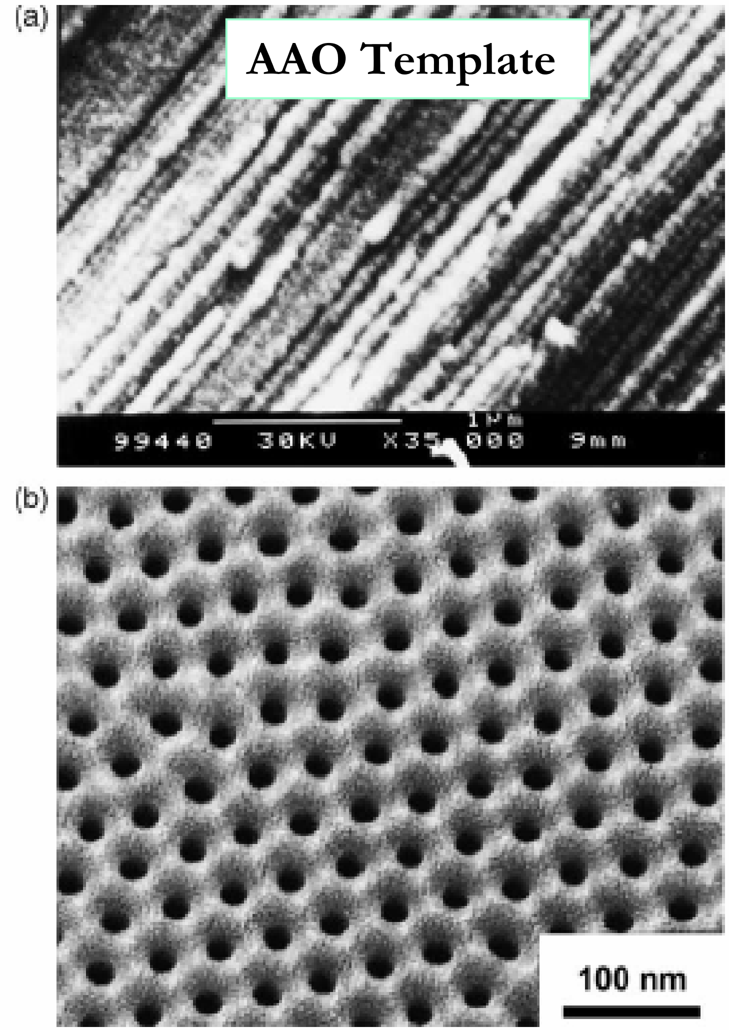

Fig. 1. SEM images of the anodic alumina oxide template with pores of 20 nm in diameter: (a) The cross section view, (b) the top view.

Annealing at 700℃ with the applied field of 10kOe. D~20nm

Hc=2500Oe ;Mr/Ms=0.9 for Co_{36}-Pb_{64} ,Ta=700 ℃

G.B. Ji et al., Solid State Commun, 132(2004)289;130(2004)541

$CoFe_2$ → $CoFe_2O4$

$CoFe_2O_4$ nanowire

$CoFe_2$

nanowire array prepared by AAO template-electrodepositio n method and further oxidization

$CoFe_2O_4$ nanowire

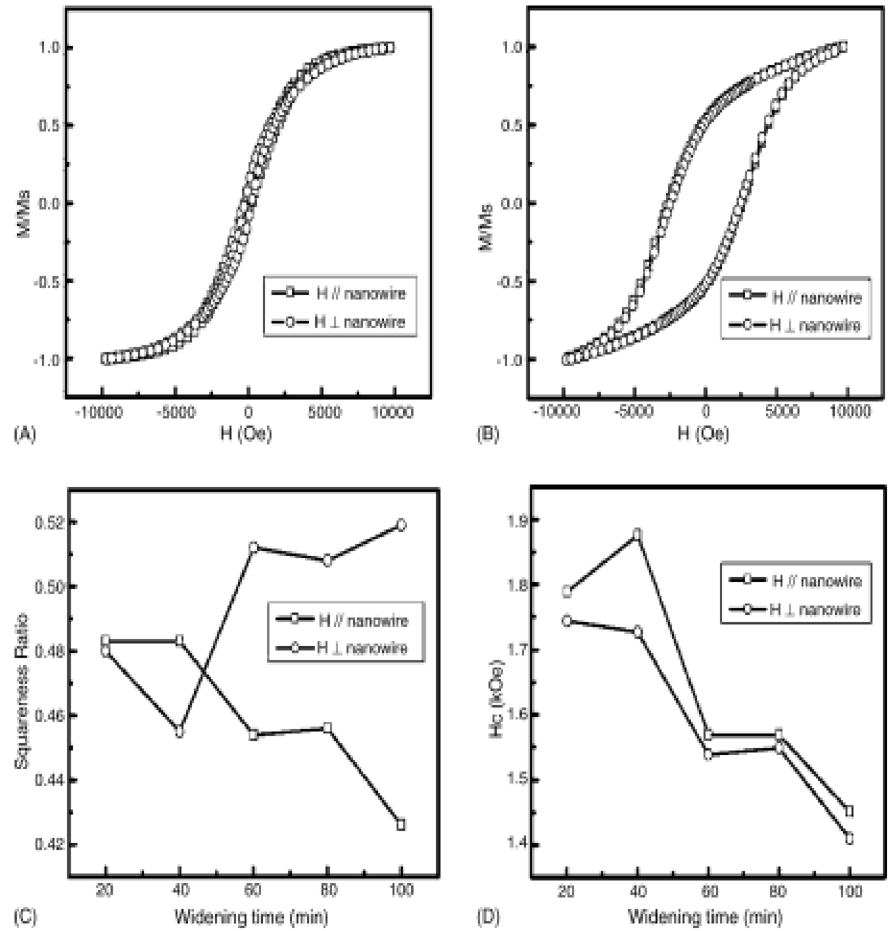

Fig. 3. Hysteresis loops of nanowire arrays (widened for 40 min): (A) $CoFe_2$ and (B) $CoFe_2O_4$. (C) Squareness ratio of $CoFe_2O_4$ nanowire arrays as a function of pore widening time. (D) H_c of $CoFe_2O_4$ nanowire arrays as a function of pore widening time. All templates were dc anodized for 8 h and deposited for 90 min. All $CoFe_2O_4$ nanowires were annealed at 620 °C for 30 h. The magnetic properties were measured with the applied field parallel and vertical to the nanowires at room temperature.

Z.H. Hua et al.,J. Alloy and Comp.427(2007)199

（Ⅳ）Magnetic Nano-film, Multlayer

- Films have been an important subject in basic and applied science.
- Thin film
- Granular film
- Multlayer

Spintronics(自旋电子学)

- Electrons have both charge and spin two degree of freedom.
- Microelectronic industry is solely based on the charge degree of freedom of electrons.
- Spintronics is a spin- based electrons .
- From physical point if enhance spin degree to the electronic devices, marvelous new devices based on the spintronics should be produced.
- The charge currents may be replaced by the spin currents in the future electronic devices.

2007年度诺贝尔物理学奖－巨磁电阻效应

Peter Grünberg（德国） Albert Fert （法国）

(1939- 5-18) (1938-3-7)

GMR—Giant Magnetoresistance

$(GaAs/001Fe/001Cr)_n$

MBE 法

Fe-磁性金属

Cr-非磁性金属

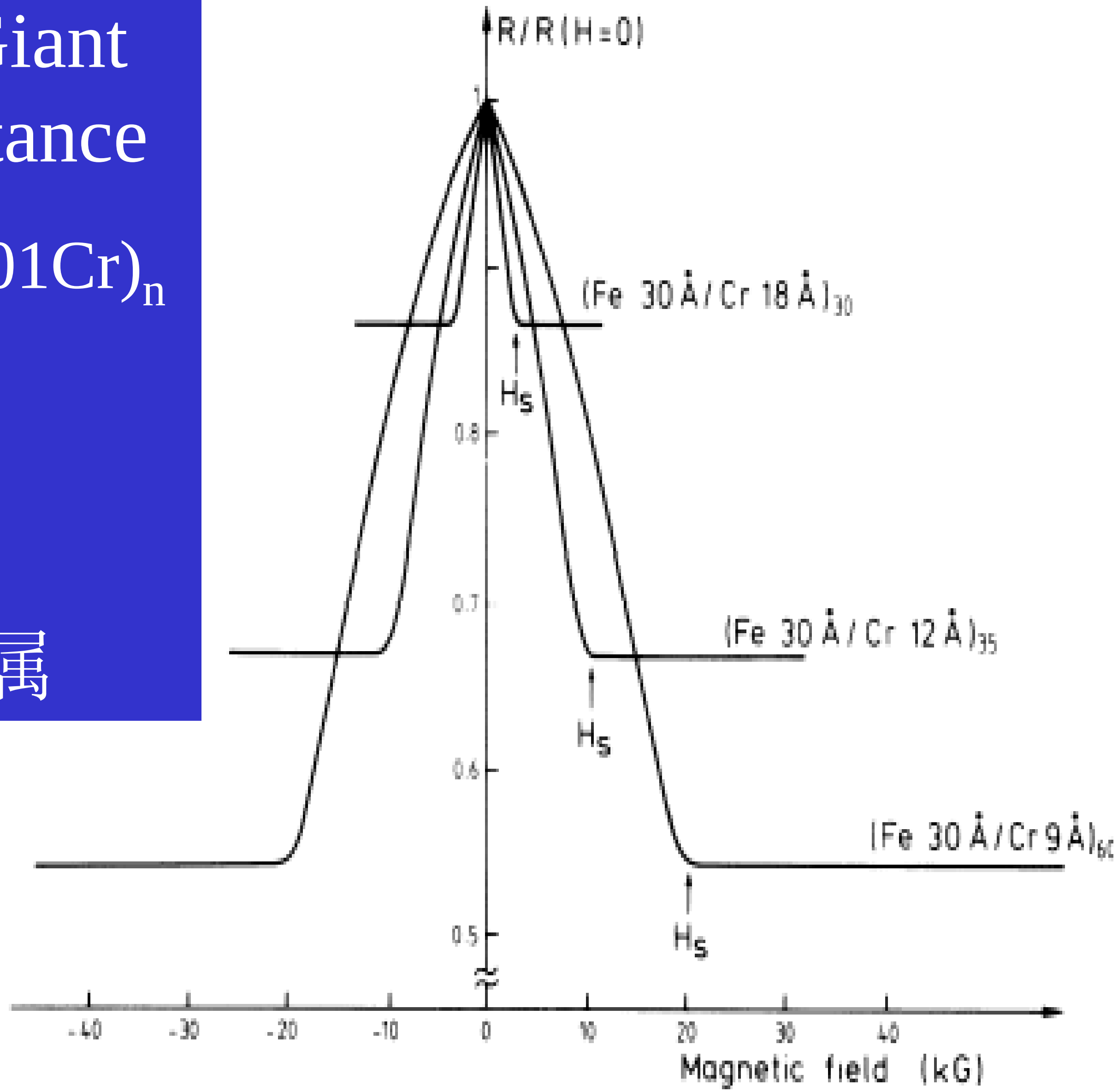

(Fe/Cr）$_n$多层膜的巨磁电阻效应

Baibich, A.Fert et al., Phys.Rev.Lett.61(1988)2472

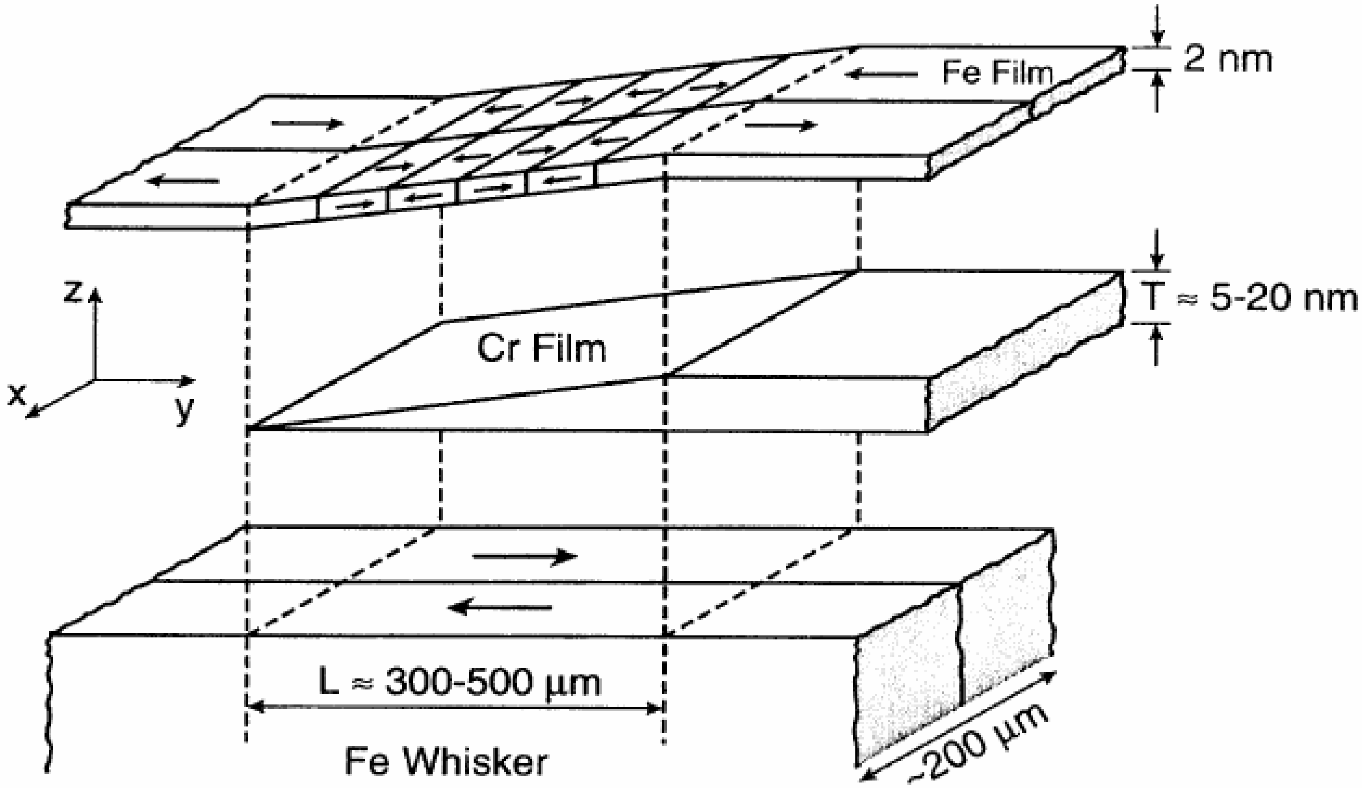

FIG. 1. A schematic exploded view of the sample structure showing the Fe(100) single-crystal whisker substrate, the evaporated Cr wedge, and the Fe overlayer. The arrows in the Fe show the direction of the magnetization in each domain. The z scale is expanded approximately 5000 times; the actual wedge angle is of order 10^{-3} deg.

J.Unguiris.et al.,Phys.Rev.Lett.,67(1991)140

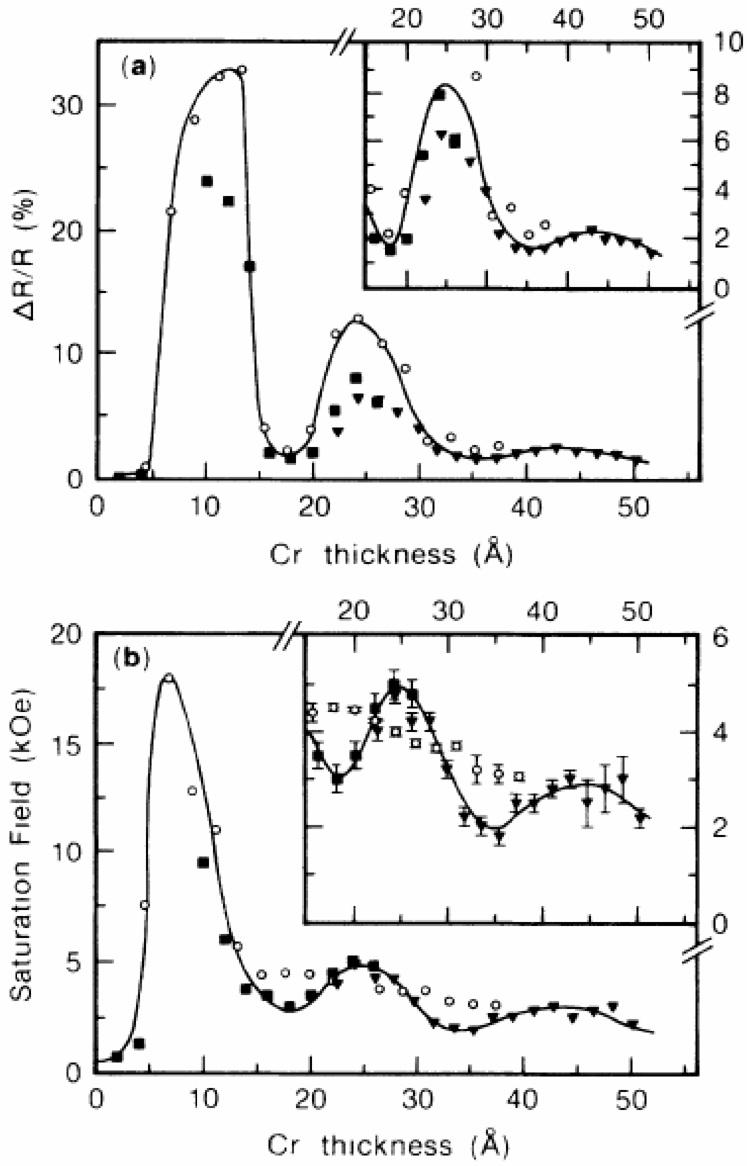

Parkin采用磁控溅射工艺制备多种具有GMR效应的多层膜。发现RKKY类型的磁电阻振荡现象。

Fe/Cr;

Co/Cr

Co/Ru

Parkin S.S.P et al., PRL,64(1990)2304

Giant Magnetoresistance

3。 巨磁电阻效应 GMR

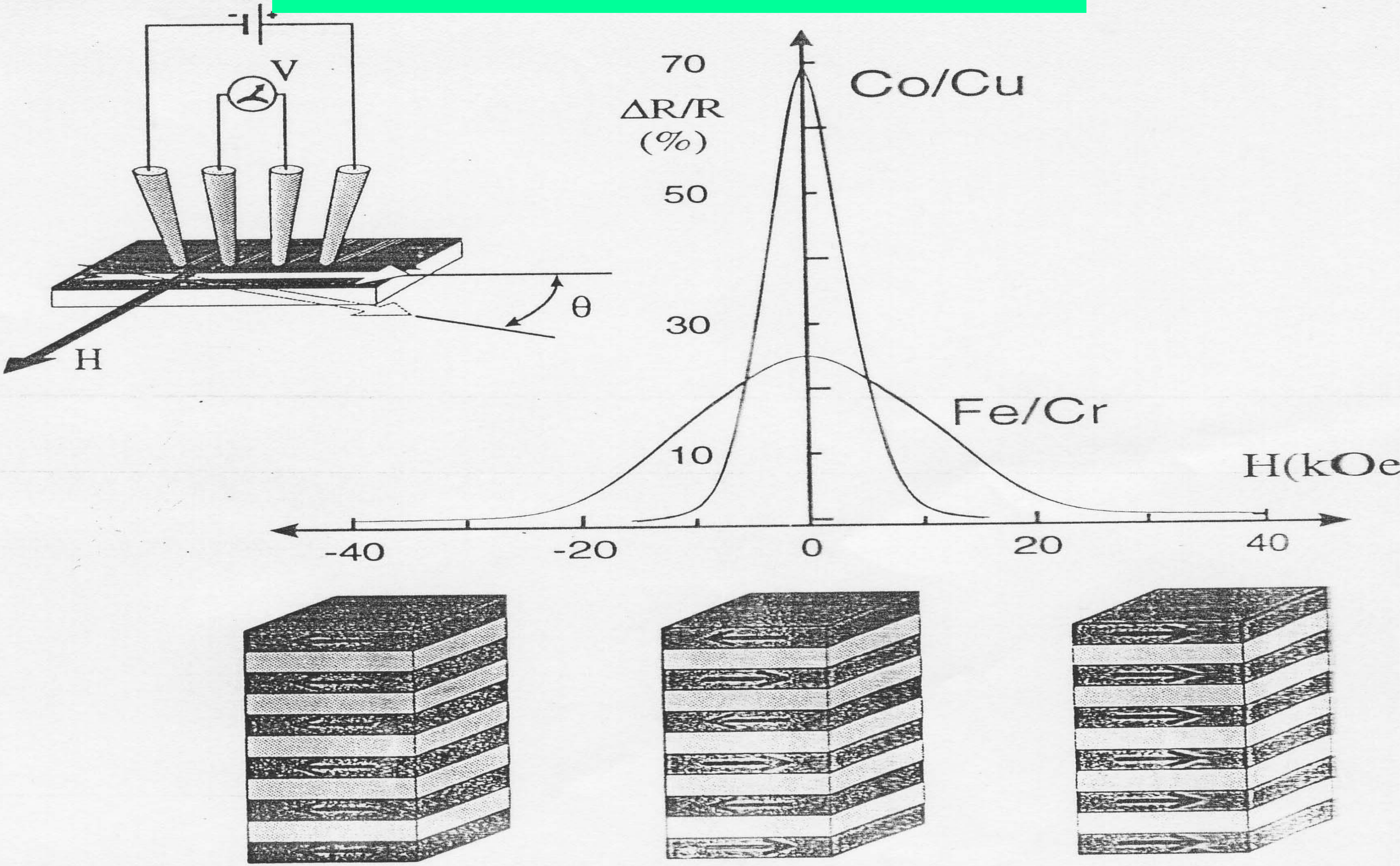

自旋阀(Spin valve)

多层膜的饱和磁场太高，磁场灵敏度低，为此采用自旋閥结构。

自由层（低矫顽力磁性薄膜，如：Ni $_{80}$Fe$_{20}$ 合金）

非磁层（如铜等非磁层薄膜）

铁磁层 （磁性薄膜,NiFe; FeCo)

钉扎层（反铁磁层，如：FeMn;MnIr)

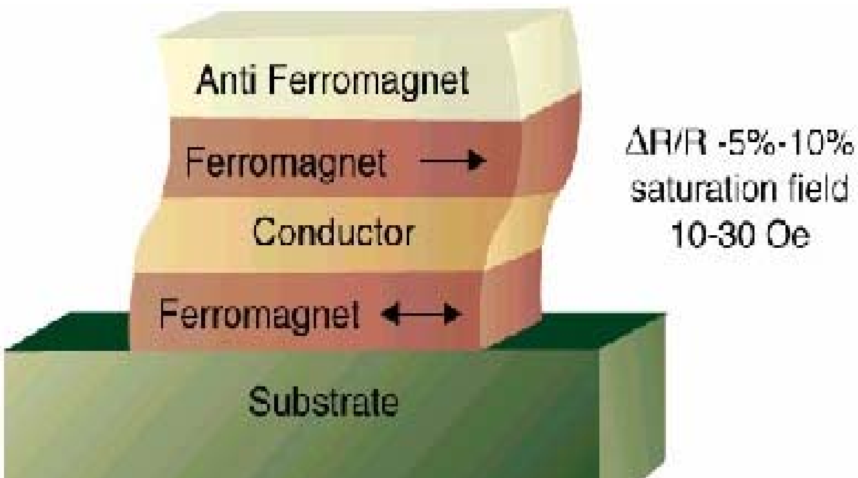

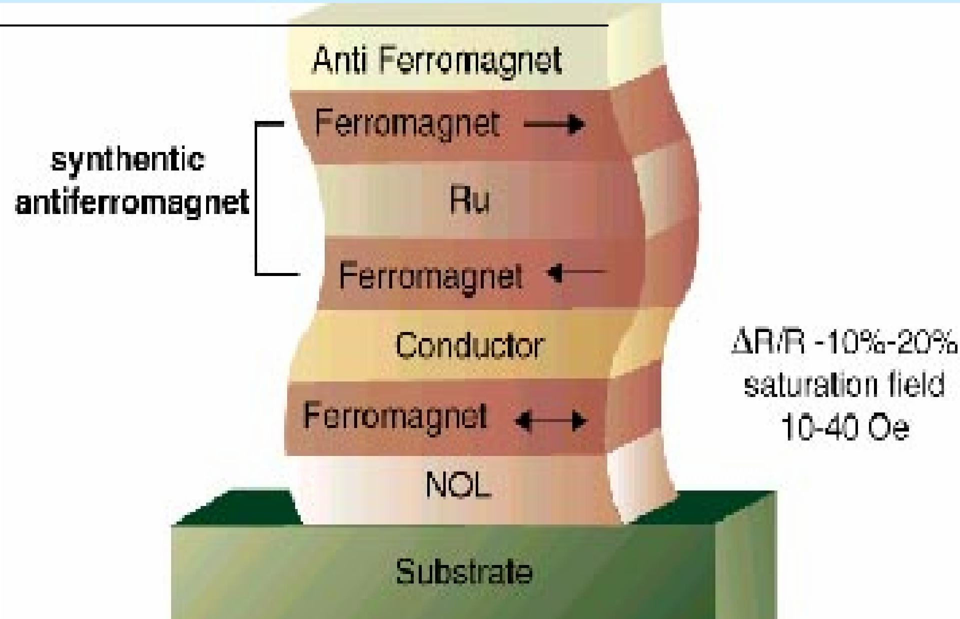

磁性材料的电子平均自由路程

$$\lambda^{\uparrow} \neq \lambda^{\downarrow}$$

λ (nm)	Fe	Co	NiFe	Cu
$\lambda^{\uparrow}$	1.5±0.2	5.5±0.4	4. 6±0.3	20.5
$\lambda^{\downarrow}$	2.1±0.5	⩽1.0	⩽0.6	20.5

对非磁性材料，如：**Cu : $\lambda^{\uparrow} = \lambda^{\downarrow} = 20.5$ nm.**

磁性材料室温自旋扩散长度($L_s = D\tau_s$)约为 50-100nm

对半导体材料，非磁金属(Cu,Au,Ag, Al etc.). Ls约为1-10 微米，有机材料也是微米量级。

如器件的尺寸与自旋扩散长度相当，自旋极化电流可以保持其

自旋取向的记忆。

自旋极化率P

$$P=(N_{\uparrow}-N_{\downarrow})/(N_{\uparrow}+N_{\downarrow})$$

Metals						
Materials	Ni	Co	Fe	$Ni_{80}Fe_{20}$	$Co_{50}Fe_{50}$	$Co_{84}Fe_{16}$
P (%)	33	45	44	48	51	49
J.S.Moodera, G.Mathon, ***J.M.M.M.***,200(1999)248-273						

Oxide Compounds			
Materials	CrO_2	Fe_3O_4	$La_{0.61}Sr_{0.23}MnO_3$
P (%)	90±3.6% [a]	40 [b]	72 [c]
[a] R.J.Soulen, ***Science***. 282 (1998)85 [b] A.Gupta, J.Z.Sun., ***J.M.M.M.***, 200(1999) 24-43 [c] D.C.Worledge and T.H.Geballe, ***Appl.Phys.Lett.*** 76(2000)900			

自旋电子学

（GMR,TMR,CMR）

磁电子学

磁电阻效应传感器

高密度磁头

MRAM

自旋晶体管

半导体自旋电子学

自旋－FET

自旋－LED

逻辑元件

量子计算机

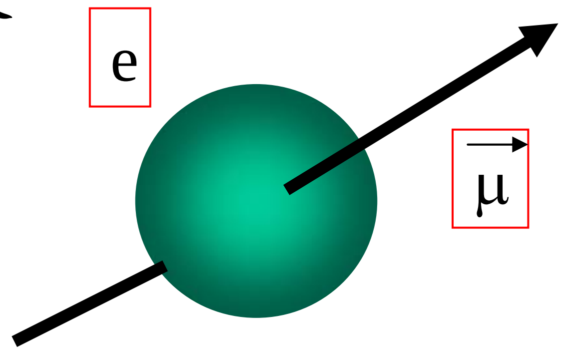

Spin-transfer-toque

宽频带微波振荡器

磁电子学

- 与自旋相关的输运性质
- 磁致电阻效应

  AMR,GMR,TMR,CMR----
- 应用

  读出磁头

  MRAM

  磁传感器

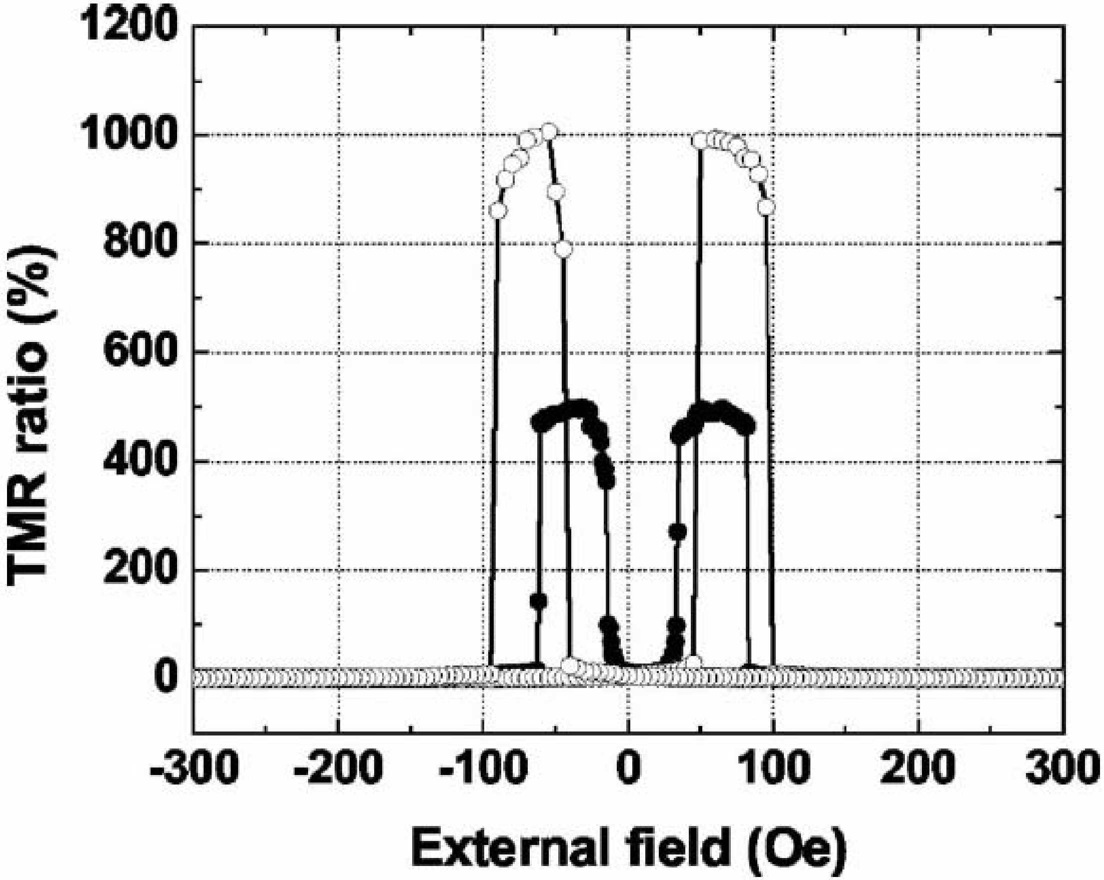

FIG. 2. TMR loops of a MTJ having 4 and 4.3 nm $(Co_{25}Fe_{75})_{80}B_{20}$ electrodes and a 2.1-nm-thick MgO annealed at 475 °C measured at RT (black circles) and 5 K (open circles).

CoFeB/MgO/CoFeB

TMR

RT:500%

5K:1010%

Lee,Y.M..et al.,A.P.L. 90(2007) 212507

硬盘记录密度的进展

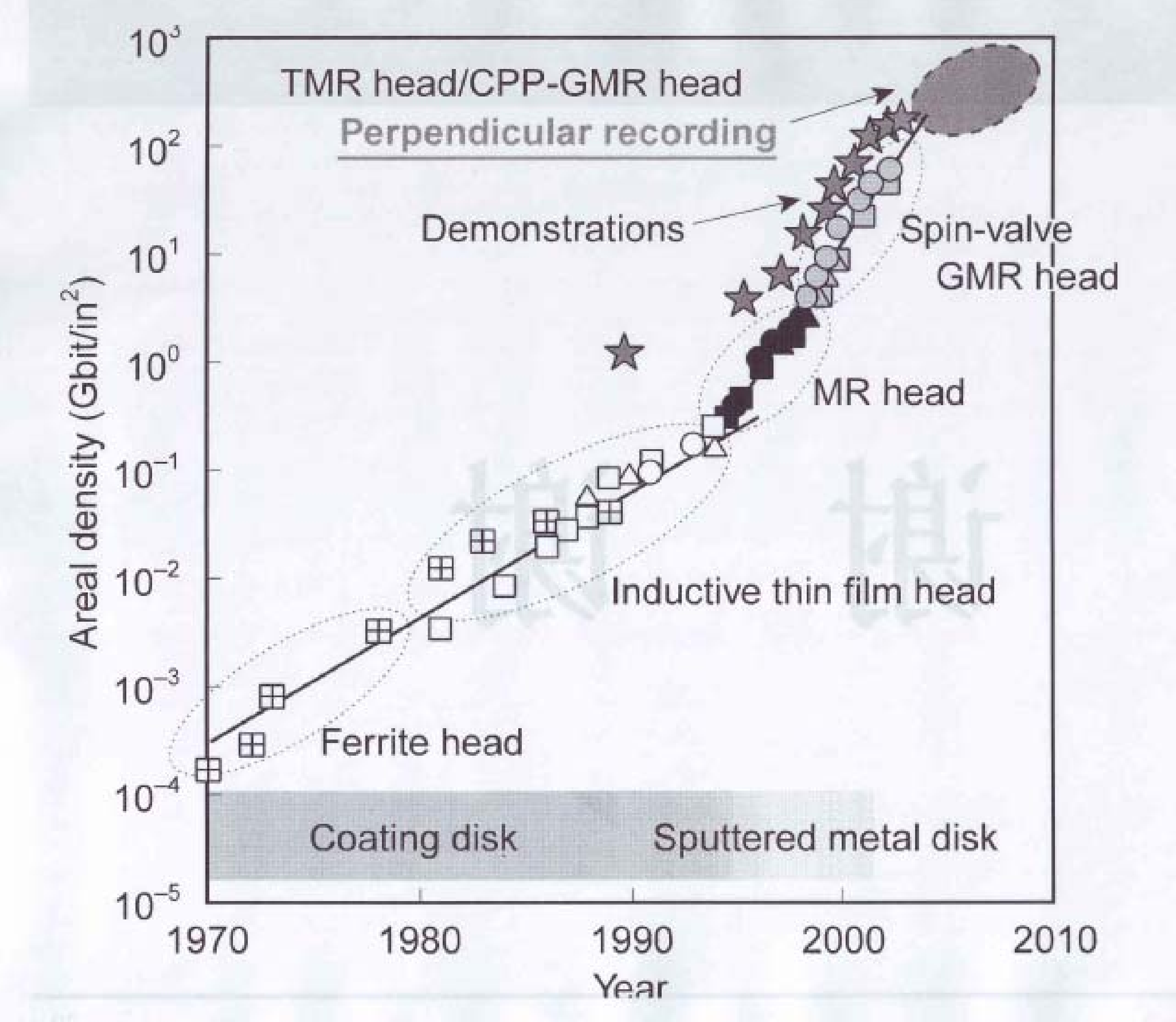

Fujitsu. Sci.Tech.j.2006,42,122

☺MRAM ; Spin Transistor

Nonvolatility, increased data processing speed, decreased electric power consumption, increased integration densities , and anti-irradiation

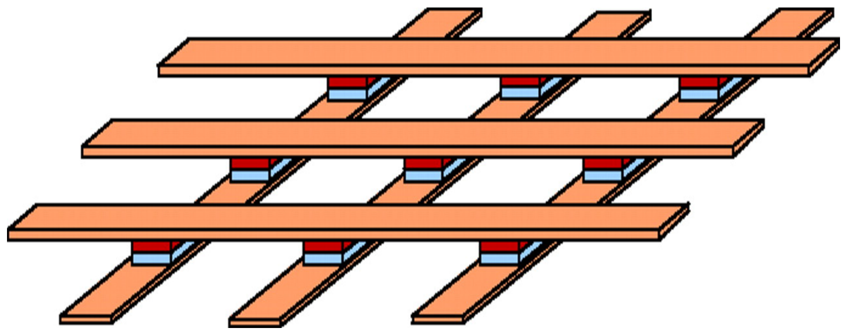

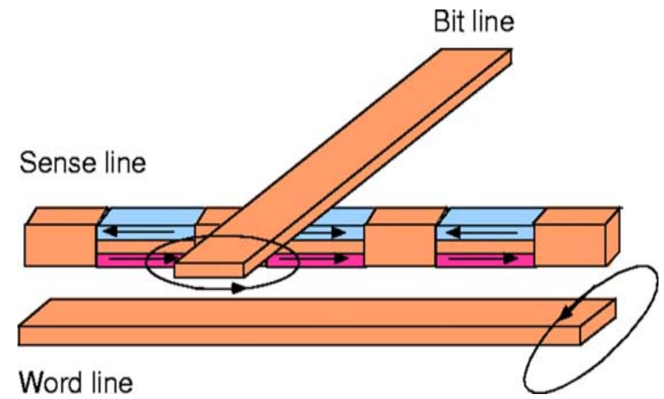

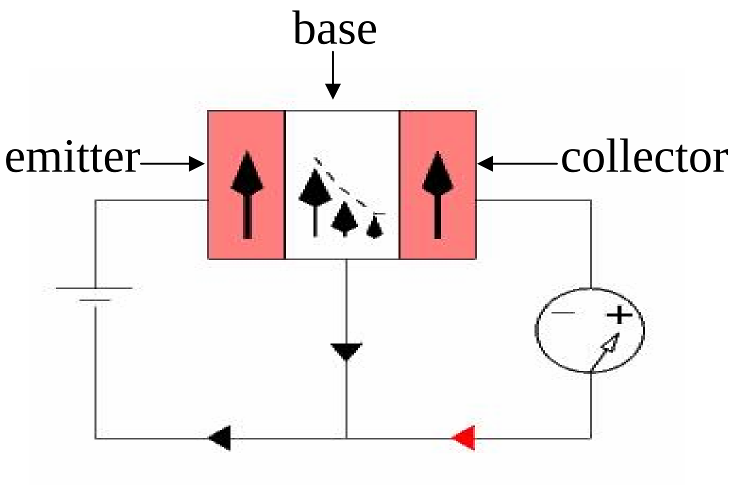

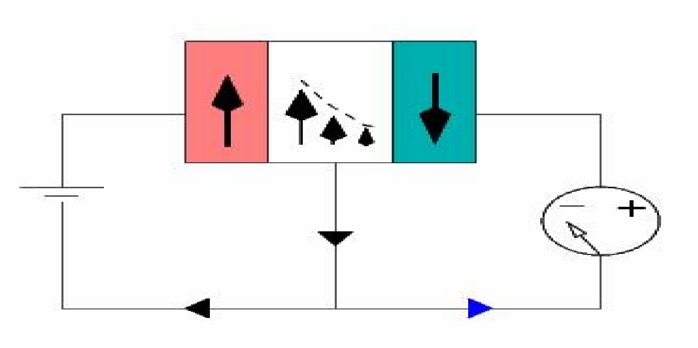

Spin transistor: three-terminal,bipolar device

MRAM—磁动态随机储存器

- 优点：非易失性；抗辐射性；高集成度；
  高运算速度；低功耗；长寿命
- 与DRAM比：非易失性；抗辐射性；高运算速度。
- 与Flash比：低功耗；长寿命；
  存取速度比Flash快千倍。
- 因此，MRAM除做内存外，尚可做外存。
- MgO绝缘层隧道结的研究成功；自旋转矩（Spin-transfer torque)的实际应用，显著加快MRAM的实用化。

MRAM: "the ideal memory", potentially combining the density of DRAM with the speed of SRAM and non-volatility of FLASH memory or hard disk, and all this while consuming a very low amount of power and has the potential to replace FLASH, DRAM and even hard-discs. MRAM can resist high radiation, and can operate in extreme temperature conditions, very suited for military and space applications.

spin-torque-transfer magnetic-random-access-memory (STT-MRAM) enter into **industrial production.**

In July 2006, Freescale started selling the first commercial MRAM module, with 4Mbit of memory, for 25$ a piece.

2008:Freescale launches independent company-EverSpin to accelerate MRAM business

Toshiba - advances in 1Gb MRAM. Expects MRAM to take over DRAM in 2015

Samsung and Hynix to launch STT-MRAM JV in September, expect the chip to mature around 2012

半导体自旋电子学

自旋注入－－极化电子的传输与控制－－检测

1。通过磁性金属多层膜的自旋注入：电阻不匹配 注入效率低于1%。

2。高自旋极化率材料的探索－－半金属材料

3。稀磁半导体材料的研究

4. 自旋霍尔效应

5. TMR, 自旋泵，自旋池，－－－

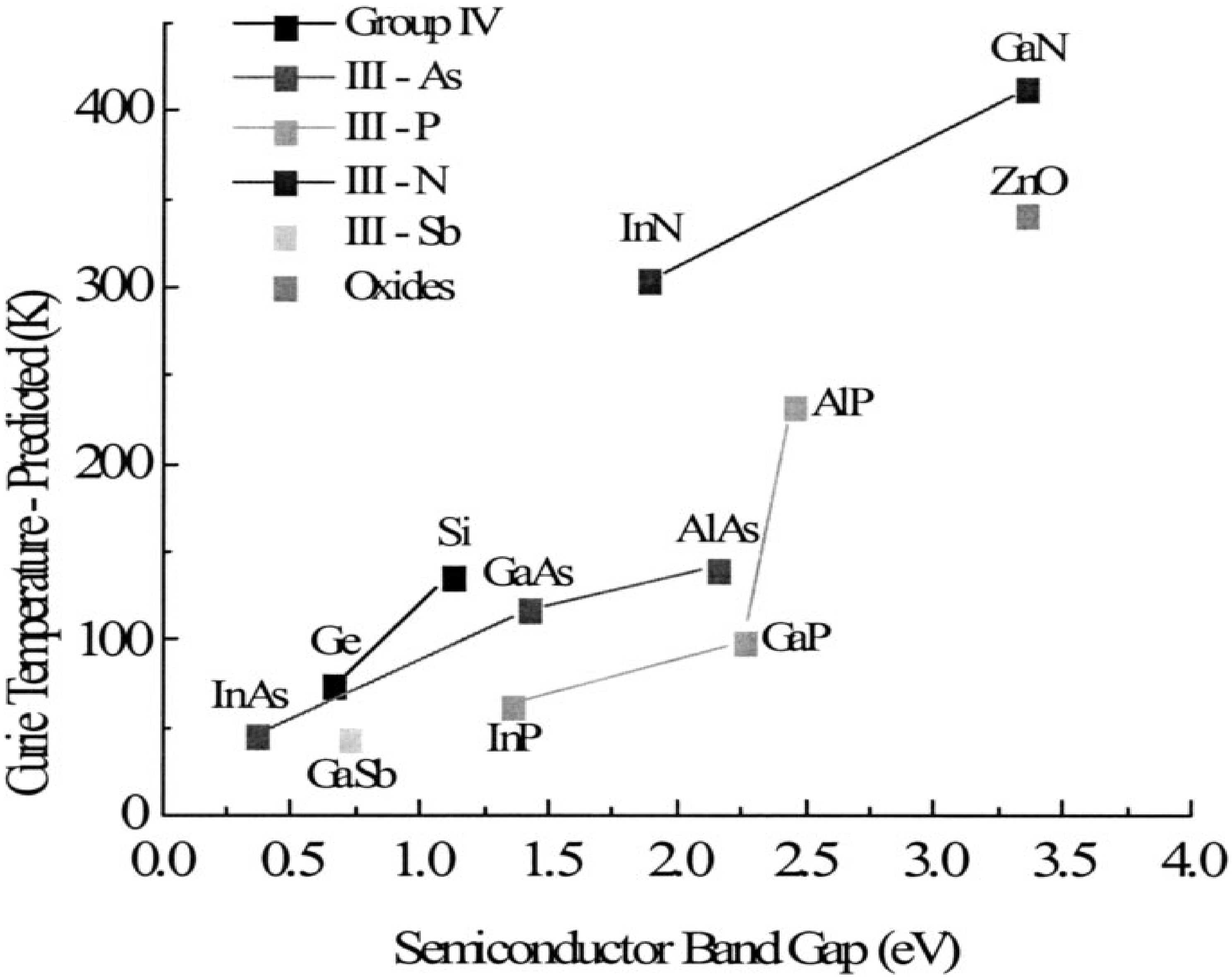

The predicted Curie temperatures as a function of the band gap

T. Dietl , et al., Science 287, (2000)1019

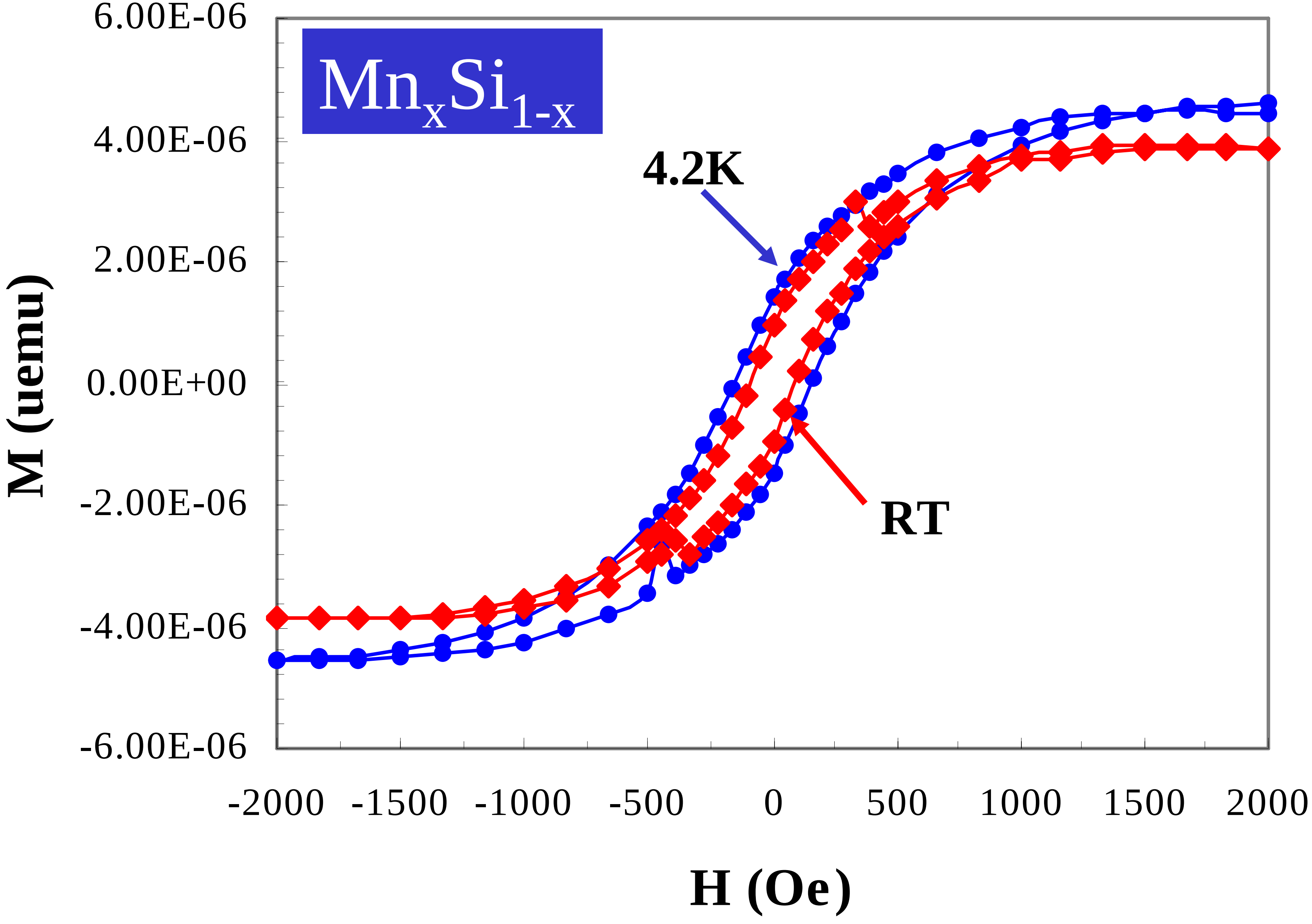

Magnetic hysteresis loops for MnSi alloy

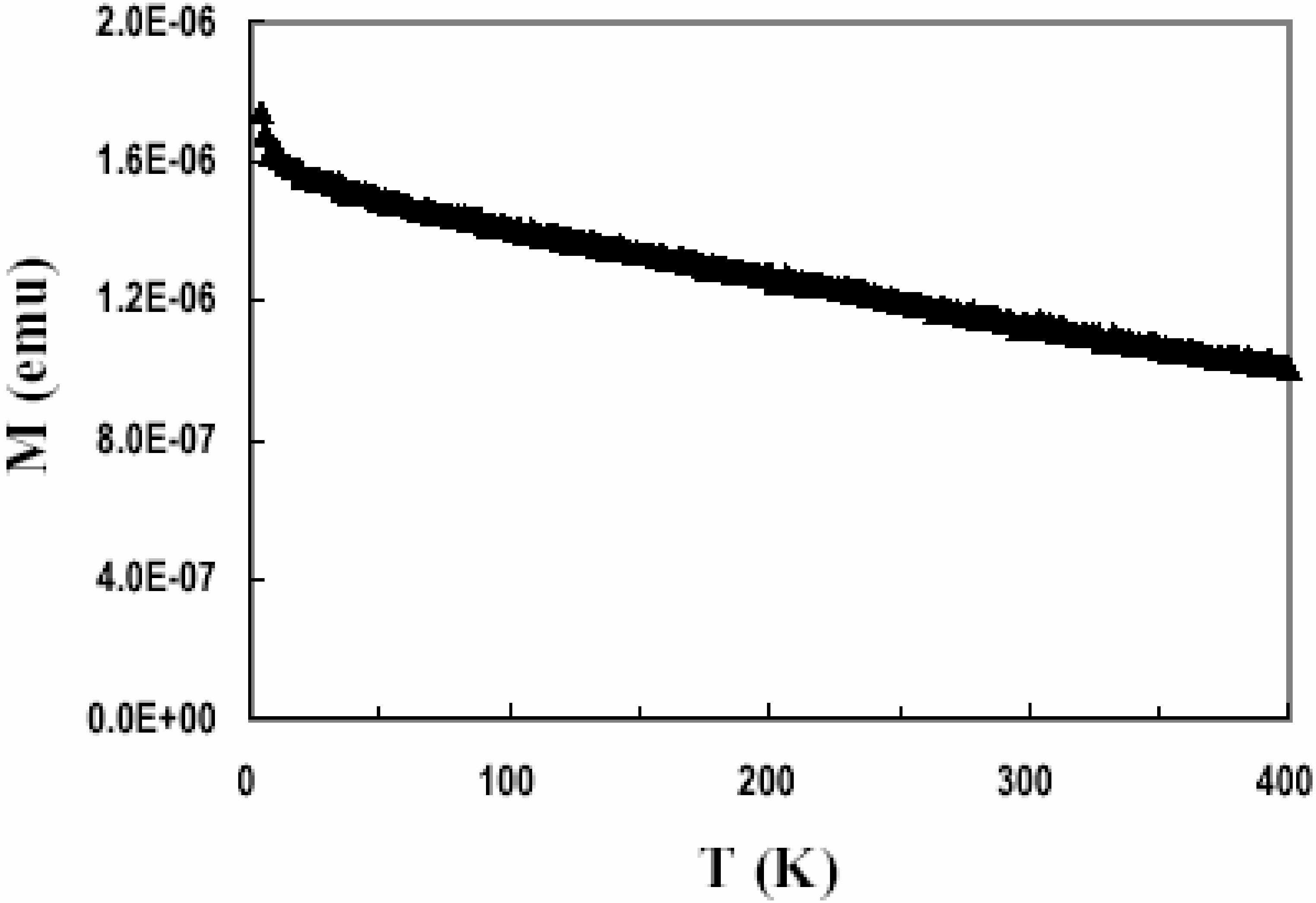
2.0E-06
1.6E-06
1.2E-06
8.0E-07
4.0E-07
0.0E+00
M (emu)
0
100
200
300
400
T (K)

Demonstration of the injection of spin into silicon

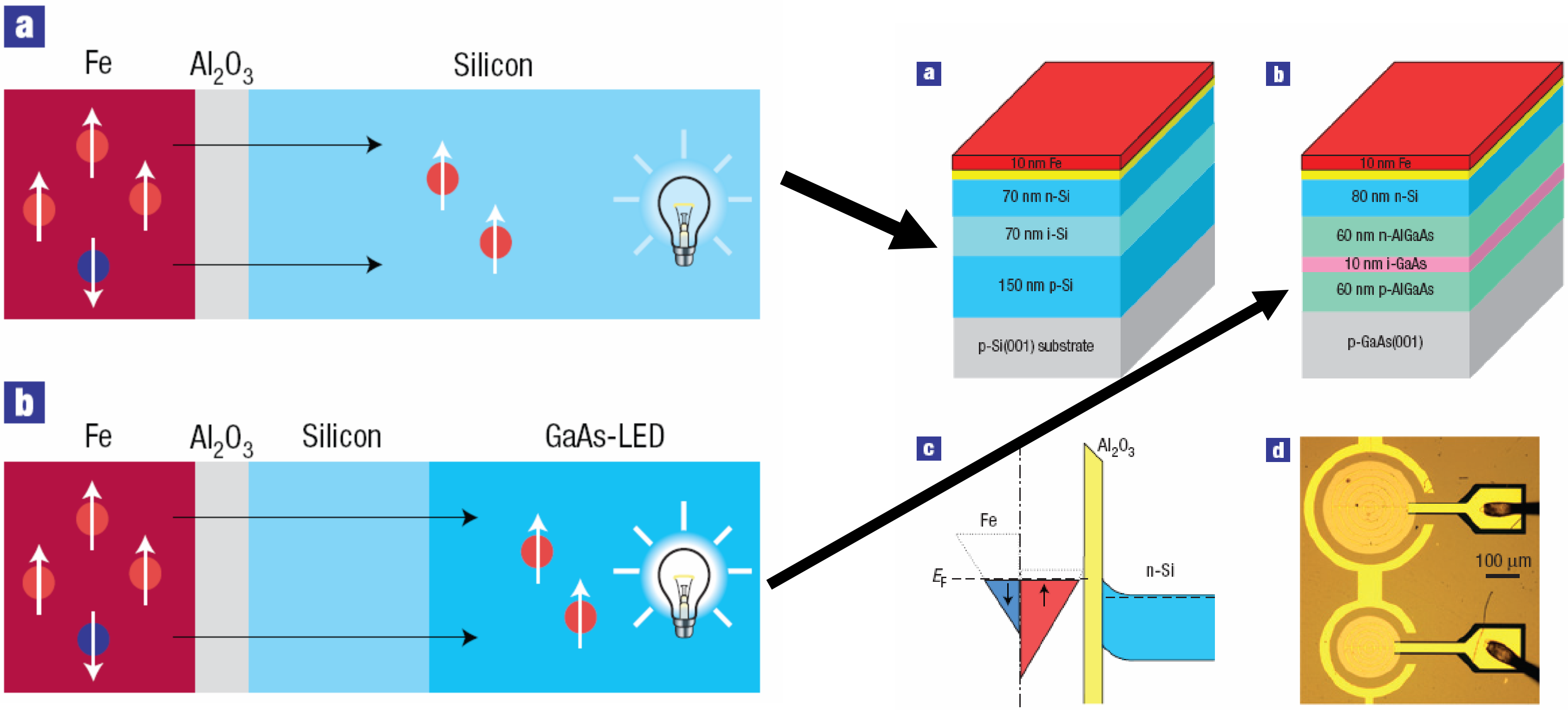

LED-Light emitting diode

R.Jansen,Nature physics,3(2007)521; B.T.Jonker,et al.,ibid,(2007)542

对稀磁半导体含义的一点看法

- 目前，稀磁半导体研究中主要是表征问题，传统的稀磁半导体概念中，磁性离子应当均匀分布在晶格中，不应形成团簇，磁性离子间应当是铁磁耦合，并产生自旋极化的磁有序。
- 该概念可拓宽为：如在非磁半导体中，掺入少量磁性原子（离子），从而产生自旋极化的现象，均可认为属稀磁半导体。这意味着即使存在磁性的团簇，只要团簇间存在相互作用，而导致自旋极化亦应归属于稀磁半导体。
- 磁性团簇在稀磁半导体中的作用值得研究。

S.J.Xiong and Y.W.Du,Physics Letters A 372(2008)2114

自旋霍尔效应

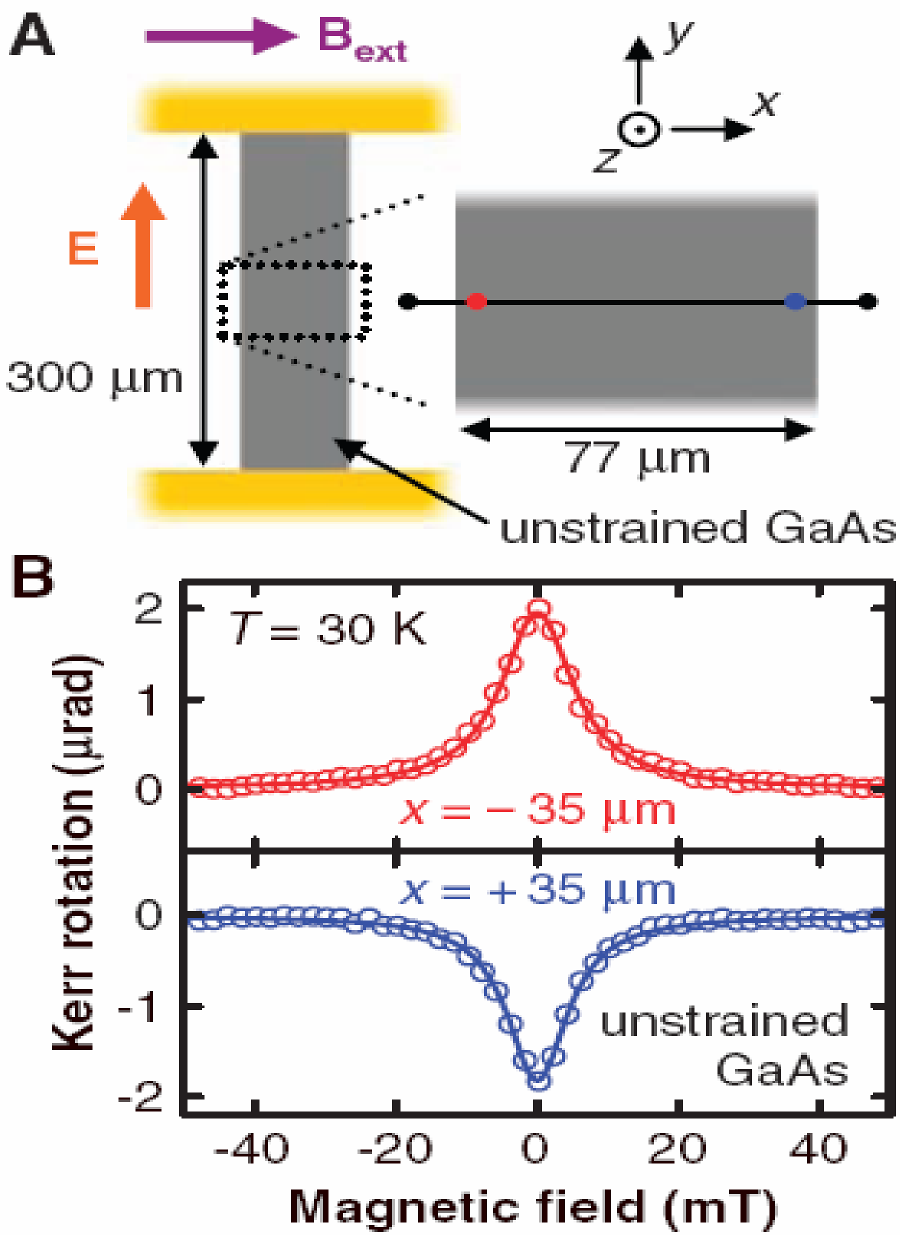

GaAs 的 Spin Hall Effect：

GaAs表面的二维电子系统，加电场后，二面产生不同自旋取向的自旋流。获Kerr效应的证实。

Kato Y.K.etal., Science。306(2004）1910

根据Rashba spin-orbit 耦合理论在高迁移率的二维电子系统，存在本征的垂直于电流方向的自旋流。

J。Sinova et al.,

PRL26(2004)126603

自旋注入到半导体中成为自旋半导体器件实用化的关键

利用GMR;TMR效应的注入由于界面自旋散射而效率甚低。

稀磁半导体作为自旋极化源前景不明朗

室温高自旋极化率的半金属尚未发现。

自旋霍尔效应有可能是自旋电子学的突破口

孙庆丰，“物理”8（2008）594。《自旋轨道耦合和自旋流的研究若干进展》

Principle of Spin Transfer Torque (STT)

STT-RAM

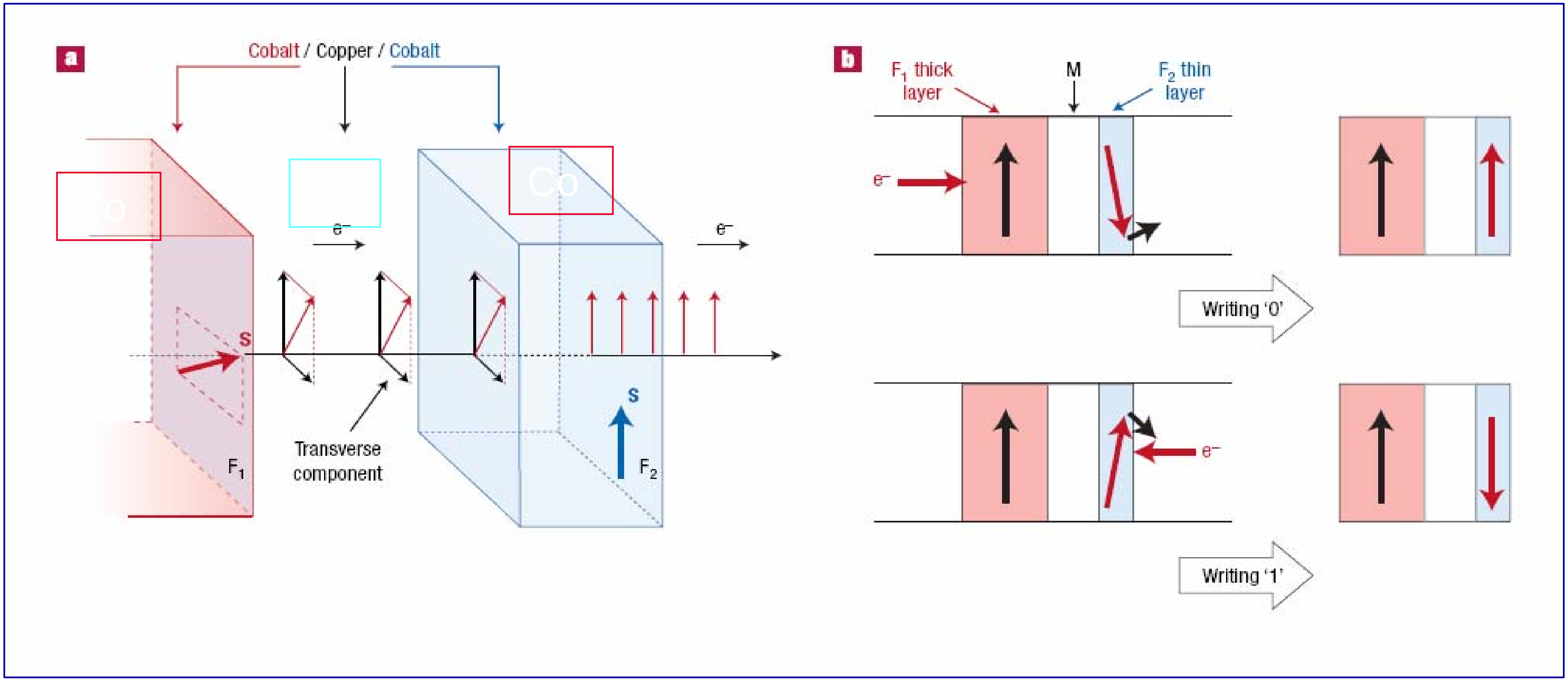

$$\frac{\partial \vec{M}(\vec{r},t)}{\partial t} = \underbrace{-|\gamma|\vec{M}\times\vec{H}_{\mathrm{eff}}}_{\text{PRECESSION}} + \underbrace{\frac{\alpha}{M_s}\vec{M}\times\frac{\partial \vec{M}}{\partial t}}_{\text{DAMPING}} + \underbrace{\frac{\sigma I}{M_s}\vec{M}\times(\vec{M}\times\vec{P})}_{\text{SPIN TRANSFER}}$$

The magnetization direction in the centre of a submicrometre mgnetic disk can now be switched by an electrical current. This discovery demonstrates the potential of realizing all-electrically controlled magnetic memory devices.

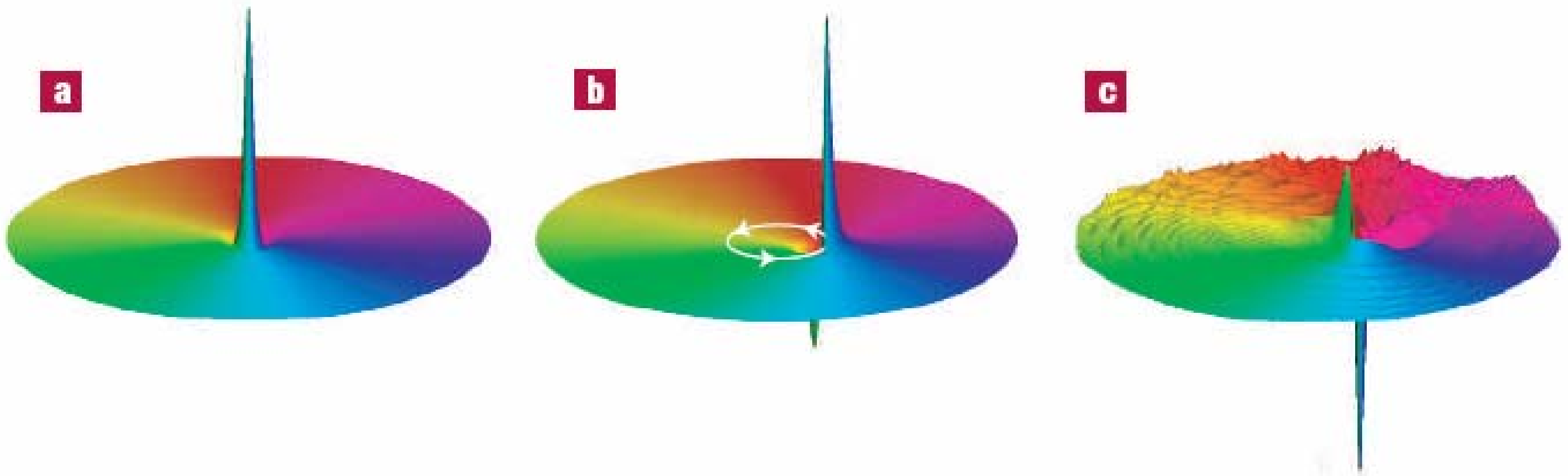

Figure 1 Magnetic vortex-core reversal. **a**, A magnetization vortex with its core shown in the centre. The height is proportional to the out-of-plane component (see text). **b**,**c**, When an oscillating electrical current is applied, the core begins to orbit the centre (**b**), and eventually switches to its other bistable state (**c**).

R.P.Cowbum, Nature Materials, 6 (2007) 255

Spin-torque oscillator-RF Device

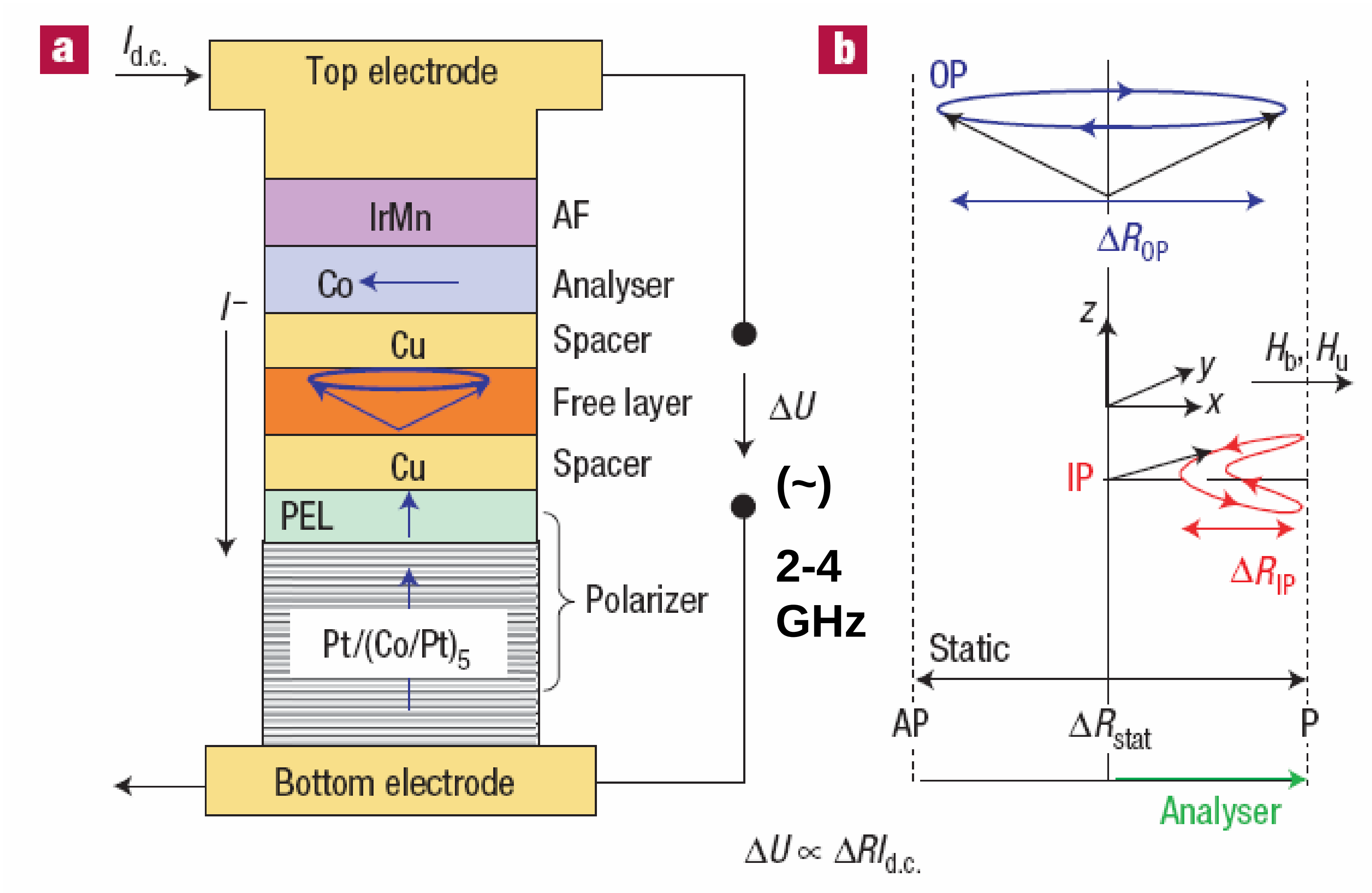

D.Houssameddine et al.,Nature materials 6(2007)447

自旋电子学是奠基在自旋基础上的电子学。微电子学仅仅利用了电子具有电荷这一自由度，从而奠定了现代信息社会的基础，如今增添了自旋这一自由度，除了电控外，尚可磁控，此外具有特殊的光学性质。因此，磁与电在固体内部的有机结合，必然会催生出一系列新颖器件的诞生，例如量子计算机中的量子比特，自旋场效应晶体管，自旋光跃迁二极管等，其影响极为深远，这是学科交叉的十分重要的研究领域。

自旋流将可能取代目前半导体元器件中的电荷流，自旋将同时肩负信息的传输、处理与存储.

20世纪也许可称为“电荷”的世纪，人们充分的调控电子具有电荷这一自由度，从而创造出从二极管直到超大规模的集成电路，奠定了信息社会的基础。本世纪也许属于“自旋”的新世纪，人们正在充分地利用、调控电子的另一个本征的自由度“自旋”，推动着社会迈向新的阶段。

谢谢